

Models of Yukawa interaction in the two Higgs doublet model, and their collider phenomenology

Mayumi Aoki,¹ Shinya Kanemura,² Koji Tsumura,³ and Kei Yagyu²

¹*Department of Physics, Tohoku University,
Aramaki, Aoba, Sendai, Miyagi 980-8578, Japan*

²*Department of Physics, University of Toyama,
3190 Gofuku, Toyama 930-8555, Japan*

³*The Abdus Salam ICTP of UNESCO and IAEA,
Strada Costiera 11, 34151 Trieste, Italy*

Abstract

Possible models of Yukawa interaction are discussed in the two Higgs doublet model (THDM) under the discrete symmetry imposed to avoid the flavor changing neutral current at the leading order. It is known that there are four types of such models corresponding to the possible different assignment of charges for the discrete symmetry on quarks and leptons. We first examine decay properties of Higgs bosons in each type model, and summarize constraints on the models from current experimental data. We then shed light on the differences among these models in collider phenomenology. In particular, we mainly discuss the so-called type-II THDM and type-X THDM. The type-II THDM corresponds to the model with the same Yukawa interaction as the minimal supersymmetric standard model. On the other hand, in the type-X THDM, additional Higgs bosons can predominantly decay into leptons. This scenario may be interesting because of the motivation for a light charged Higgs boson scenario such as in the TeV scale model of neutrino, dark matter and baryogenesis. We study how we can distinguish the type-X THDM from the minimal supersymmetric standard model at the Large Hadron Collider and the International Linear Collider.

PACS numbers: 12.60.Fr, 14.80.Cp, 14.60.-z

Keywords:

I. INTRODUCTION

The CERN LHC, which is a proton-proton collider with maximal energy 14 TeV, has started its operation [1]. The most important purpose of the LHC is hunting for the Higgs boson, the last unknown particle in the standard model (SM). The Higgs sector is introduced for the spontaneous breakdown of the electroweak gauge symmetry. Weak gauge bosons (W^\pm and Z) then receive their masses via the Higgs mechanism, and quarks and charged leptons receive their masses through the Yukawa interaction. Because the SM Higgs sector has not been confirmed yet, the possibility of its non-minimal form should also be considered in order to understand the nature of the symmetry breaking. In fact, it is well known that many candidates of physics beyond the SM predict extended Higgs sectors. For example, supersymmetric extensions of the SM have at least two Higgs doublets [2]. Successful models based on dynamical symmetry breaking also may require the non-minimal form as the Higgs sector in the low energy effective theory [3]. In addition, some of new physics models that are intended to solve the problems which the SM cannot explain, such as tiny neutrino masses, essence of dark matter, and baryogenesis, has been built with the extension of the electroweak symmetry breaking sector [4, 5, 6, 7].

There are two basic experimental constraints which an extended Higgs sector must respect: those on the electroweak rho parameter (ρ) as well as the flavour changing neutral current (FCNC). The measured value of the rho parameter ($\rho_{\text{exp}} \approx 1$) suggest that the electroweak sector of the model would approximately have a global $SU(2)$ symmetry (the custodial symmetry) which guarantees $\rho = 1$ at tree level [8]. For this to be satisfied, a possibility of the structure with (multi-) isospin doublets (plus singlets) would be natural as the Higgs sector. In the SM, FCNC phenomena are suppressed due to the electromagnetic gauge symmetry and due to the Glashow-Iliopoulos-Maiani mechanism [9], so that the experimental bounds on the FCNC processes are satisfied. In models with more than one Higgs doublet, this is not true in general, because two or more Yukawa matrices for each fermion cannot be simultaneously diagonalized. It is well known that, to avoid such Higgs-boson-associated FCNC interactions, each fermion should couple to only one of the Higgs doublets. This can be realized in a natural way by imposing a discrete Z_2 symmetry [10].

In this paper, we discuss phenomenological differences in various models of Yukawa interactions under the discrete Z_2 symmetry in the two Higgs doublet model (THDM). It has

been known that there are four patterns of the Yukawa interaction depending on the assignment of charges for quarks and leptons under the Z_2 symmetry [11, 12, 13]. We refer them as type-I, type-II, type-X and type-Y THDMs¹. The type in the Yukawa interaction can be related to the new physics scenarios. For example, the Higgs sector of the minimal supersymmetric standard model (MSSM) is the THDM with a supersymmetric relation [2] among the parameters of the Higgs sector, whose Yukawa interaction is of type-II, in which only a Higgs doublet couples to up-type quarks and the other couples to down-type quarks and charged leptons. On the other hand, a TeV scale model to try to explain neutrino masses, dark matter and baryogenesis has been proposed in Ref. [7]. In this model the Higgs sector is the two Higgs doublets with extra scalar singlets, and the Yukawa interaction corresponds to the type-X, in which only a Higgs doublet couples to quarks, and the other couples to leptons. Therefore, in order to select the true model from various new physics candidates that predict THDMs (and their variations with singlets), it is important to experimentally determine the type of the Yukawa interaction.

There have been many studies for the phenomenological properties of the type-II THDM, often in the context of the MSSM [2]. On the contrary, there has been fewer studies for the other types of Yukawa interactions in the THDM. The purpose of this paper is to clarify phenomenological differences among these types of Yukawa interactions in the THDM at the LHC and the International Linear Collider (ILC) [15]. We first study the decay rates and the decay branching ratios of the CP-even (h and H) and CP-odd (A) neutral Higgs bosons and the charged Higgs bosons (H^\pm) in various types of Yukawa interactions. It is confirmed that there are large differences in the Higgs boson decays among these types of Yukawa interactions in the THDM. In particular, in the case where the CP-even Higgs boson h is approximately SM-like, H and A decay mainly into $\tau^+\tau^-$ in the type-X scenario for the wide range of parameter space, while they decay mainly into $b\bar{b}$ in the type-II scenario. We then summarize constraints on the mass of H^\pm from current experimental bounds in various types of Yukawa interactions. In addition to the lower bounds on the mass (m_{H^\pm}) from CERN LEP and Tevatron direct searches [16, 17], m_{H^\pm} can also be constrained by the B -meson

¹ The type-X (type-Y) THDM is referred to as type-IV (type-III) THDM in Ref. [11] and the type-I' (type-II') THDM in Ref. [12]. Sometimes the most general THDM, in which each fermion couples to both Higgs doublet fields, is called the type-III [14]. To avoid confusion we just call them as these type-X and type-Y THDMs.

decay data such as $B \rightarrow X_s \gamma$ [18, 19, 20, 21] and $B \rightarrow \tau \nu$ [22, 23], depending on the model of Yukawa interaction. The $B \rightarrow X_s \gamma$ results give a severe lower bound, $m_{H^\pm} \gtrsim 295$ GeV, at the next-to-next-to-leading order (NNLO) in the (non-supersymmetric) type-II THDM and the type-Y THDM [20, 21], but provide no effective bound in the type-I (type-X) THDM for $\tan \beta \gtrsim 2$, where $\tan \beta$ is the ratio of the vacuum expectation values (VEVs) of the CP-even Higgs bosons. We also discuss the experimental bounds on the charged Higgs sector from purely leptonic observables $\tau \rightarrow \mu \bar{\nu} \nu$ [24] and the muon anomalous magnetic moment [25, 26].

We finally discuss the possibility of discriminating between the types of Yukawa interactions at the LHC and also at the ILC. We mainly study collider phenomenology in the type-X THDM in the light extra Higgs boson scenario, and see differences from the results in the MSSM (the type-II THDM). We discuss the signal of neutral and charged Higgs bosons at the LHC, which may be useful to distinguish the type of the Yukawa interaction. The feasibility of the direct production processes from gluon fusion $gg \rightarrow A$ (H) and the associated production from $pp \rightarrow b\bar{b}A$ ($b\bar{b}H$) is studied and the difference in the signal significance of their leptonic decay channels is evaluated in the type-X THDM and the MSSM. We also consider the Higgs boson pair production $pp \rightarrow AH^\pm, HH^\pm, AH$ and find that the leptonic decay modes are also useful to explore the type of the Yukawa interaction. At the ILC, the process of $e^+e^- \rightarrow AH$ is useful to examine the type-X THDM, because the final states are completely different from the case of the MSSM.

In Sec. II, we give a brief review of the types of the Yukawa interactions in the THDM. In Sec. III, the decay widths and the branching ratios are evaluated in the four different types of the Yukawa interactions. Section IV is devoted to a discussion of current experimental constraints on the THDM in each type of the Yukawa interaction. In Sec. V, the possibility of discriminating the type of the Yukawa interaction at the LHC and the ILC is discussed. Conclusions are given in Sec. VI. The formulae of the decay rates of the Higgs bosons are listed in the Appendix.

II. TWO HIGGS DOUBLET MODELS UNDER THE Z_2 SYMMETRY

In the THDM with isospin doublet scalar fields Φ_1 and Φ_2 with a hypercharge of $Y = 1/2$, the discrete Z_2 symmetry ($\Phi_1 \rightarrow \Phi_1$ and $\Phi_2 \rightarrow -\Phi_2$) may be imposed to avoid FCNC at

	Φ_1	Φ_2	u_R	d_R	ℓ_R	Q_L, L_L
Type-I	+	-	-	-	-	+
Type-II	+	-	-	+	+	+
Type-X	+	-	-	-	+	+
Type-Y	+	-	-	+	-	+

TABLE I: Variation in charge assignments of the Z_2 symmetry.

the lowest order [10]. The most general Yukawa interaction under the Z_2 symmetry can be written as

$$\mathcal{L}_{\text{yukawa}}^{\text{THDM}} = -\overline{Q}_L Y_u \tilde{\Phi}_u u_R - \overline{Q}_L Y_d \Phi_d d_R - \overline{L}_L Y_\ell \Phi_\ell \ell_R + \text{H.c.}, \quad (1)$$

where Φ_f ($f = u, d$ or ℓ) is either Φ_1 or Φ_2 . There are four independent Z_2 charge assignments on quarks and charged leptons, as summarized in TABLE I [11, 12]. In the type-I THDM, all quarks and charged leptons obtain their masses from the VEV of Φ_2 . In the type-II THDM, masses of up-type quarks are generated by the VEV of Φ_2 , while those of down-type quarks and charged leptons are acquired by that of Φ_1 . The Higgs sector of the MSSM is a special THDM whose Yukawa interaction is of type-II. The type-X Yukawa interaction (all quarks couple to Φ_2 while charged leptons couple to Φ_1) is used in the model in Ref. [7]. The remaining one is referred to as the type-Y THDM.

The most general Higgs potential under the softly broken Z_2 symmetry is given by

$$V^{\text{THDM}} = m_1^2 \Phi_1^\dagger \Phi_1 + m_2^2 \Phi_2^\dagger \Phi_2 - m_3^2 (\Phi_1^\dagger \Phi_2 + \Phi_2^\dagger \Phi_1) + \frac{\lambda_1}{2} (\Phi_1^\dagger \Phi_1)^2 + \frac{\lambda_2}{2} (\Phi_2^\dagger \Phi_2)^2 \\ + \lambda_3 (\Phi_1^\dagger \Phi_1) (\Phi_2^\dagger \Phi_2) + \lambda_4 (\Phi_1^\dagger \Phi_2) (\Phi_2^\dagger \Phi_1) + \frac{\lambda_5}{2} [(\Phi_1^\dagger \Phi_2)^2 + (\Phi_2^\dagger \Phi_1)^2], \quad (2)$$

where the parameters m_3^2 and λ_5 are complex, in general. In this paper, they are taken to be real by assuming CP invariance. The Higgs doublet fields can be parametrized as

$$\Phi_i = \begin{pmatrix} \omega_i^+ \\ \frac{1}{\sqrt{2}}(v_i + h_i - i z_i) \end{pmatrix}, \quad (3)$$

and the mass eigenstates are defined by

$$\begin{pmatrix} h_1 \\ h_2 \end{pmatrix} = R(\alpha) \begin{pmatrix} H \\ h \end{pmatrix}, \quad \begin{pmatrix} z_1 \\ z_2 \end{pmatrix} = R(\beta) \begin{pmatrix} z \\ A \end{pmatrix}, \quad \begin{pmatrix} \omega_1^+ \\ \omega_2^+ \end{pmatrix} = R(\beta) \begin{pmatrix} \omega^+ \\ H^+ \end{pmatrix}, \quad (4)$$

	ξ_h^u	ξ_h^d	ξ_h^ℓ	ξ_H^u	ξ_H^d	ξ_H^ℓ	ξ_A^u	ξ_A^d	ξ_A^ℓ
Type-I	c_α/s_β	c_α/s_β	c_α/s_β	s_α/s_β	s_α/s_β	s_α/s_β	$\cot \beta$	$-\cot \beta$	$-\cot \beta$
Type-II	c_α/s_β	$-s_\alpha/c_\beta$	$-s_\alpha/c_\beta$	s_α/s_β	c_α/c_β	c_α/c_β	$\cot \beta$	$\tan \beta$	$\tan \beta$
Type-X	c_α/s_β	c_α/s_β	$-s_\alpha/c_\beta$	s_α/s_β	s_α/s_β	c_α/c_β	$\cot \beta$	$-\cot \beta$	$\tan \beta$
Type-Y	c_α/s_β	$-s_\alpha/c_\beta$	c_α/s_β	s_α/s_β	c_α/c_β	s_α/s_β	$\cot \beta$	$\tan \beta$	$-\cot \beta$

TABLE II: The mixing factors in Yukawa interactions in Eq. (6)

where the rotation matrix is given by

$$R(\theta) = \begin{pmatrix} \cos \theta & -\sin \theta \\ \sin \theta & \cos \theta \end{pmatrix}. \quad (5)$$

There are five physical Higgs bosons, i.e., two CP-even states h and H , one CP-odd state A , and a pair of charged states H^\pm , and z and ω^\pm are Nambu-Goldstone bosons that are eaten as the longitudinal components of the massive gauge bosons. The eight parameters m_1^2 – m_3^2 and λ_1 – λ_5 in the Higgs sector are replaced by eight physical parameters: i.e., the VEV $v = \sqrt{v_1^2 + v_2^2} \simeq 246$ GeV, the mixing angles α and β ($\tan \beta = v_2/v_1$), the Higgs boson masses m_h, m_H, m_A, m_{H^\pm} , and the soft breaking mass parameter $M = m_3/\sqrt{\sin \beta \cos \beta}$. The mixing angle α is defined such that h is the SM-like Higgs boson when $\sin(\beta - \alpha) = 1$.

The Yukawa interactions are expressed in terms of mass eigenstates of the Higgs bosons as

$$\begin{aligned} \mathcal{L}_{\text{yukawa}}^{\text{THDM}} = & - \sum_{f=u,d,\ell} \left(\frac{m_f}{v} \xi_h^f \bar{f} f h + \frac{m_f}{v} \xi_H^f \bar{f} f H - i \frac{m_f}{v} \xi_A^f \bar{f} \gamma_5 f A \right) \\ & - \left\{ \frac{\sqrt{2} V_{ud}}{v} \bar{u} (m_u \xi_A^u P_L + m_d \xi_A^d P_R) d H^+ + \frac{\sqrt{2} m_\ell \xi_A^\ell}{v} \bar{\nu}_L \ell_R H^+ + \text{H.c.} \right\}, \quad (6) \end{aligned}$$

where $P_{L/R}$ are projection operators for left-/right-handed fermions, and the factors ξ_φ^f are listed in TABLE II.

For the successful electroweak symmetry breaking, a combination of quartic coupling constants should satisfy the condition of vacuum stability [27, 28]. We also take into account bounds from perturbative unitarity [29] to restrict parameters in the Higgs potential [30, 31]. The top and bottom Yukawa coupling constants cannot be taken too large. The requirement $|Y_{t,b}|^2 < \pi$ at the tree level can provide a milder constraint $0.4 \lesssim \tan \beta \lesssim 91$, where $|Y_t| = (\sqrt{2}/v) m_t \cot \beta$ and $|Y_b| = (\sqrt{2}/v) m_b \tan \beta$.

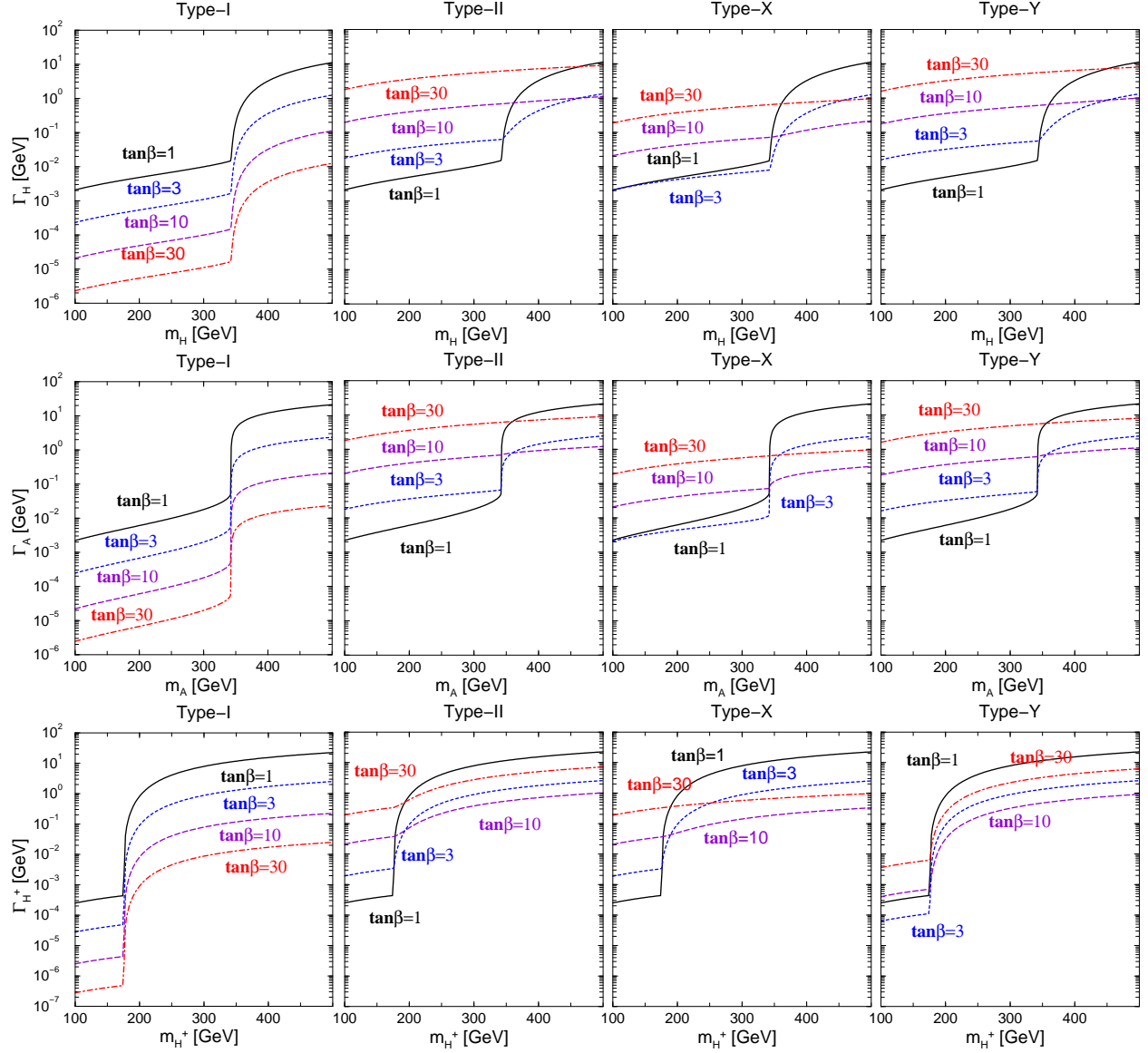


FIG. 1: Total decay widths of H , A and H^\pm in the four different types of THDM as a function of the decaying scalar boson mass for several values of $\tan \beta$ under the assumption $m_\Phi = m_H = m_A = m_{H^\pm}$ and $M = m_\Phi - 1$ GeV. The SM-like limit $\sin(\beta - \alpha) = 1$ is taken, where h is the SM-like Higgs boson.

III. DECAYS OF HIGGS BOSONS

In this section, we discuss the difference in decays of the Higgs bosons for the types of Yukawa interactions in the THDM. We calculate the decay rates of the Higgs bosons and evaluate the total widths and the branching ratios. In particular, we show the result with $\sin(\beta - \alpha) \simeq 1$ [32, 33], where h is the SM-like Higgs boson while the VEV of H is very

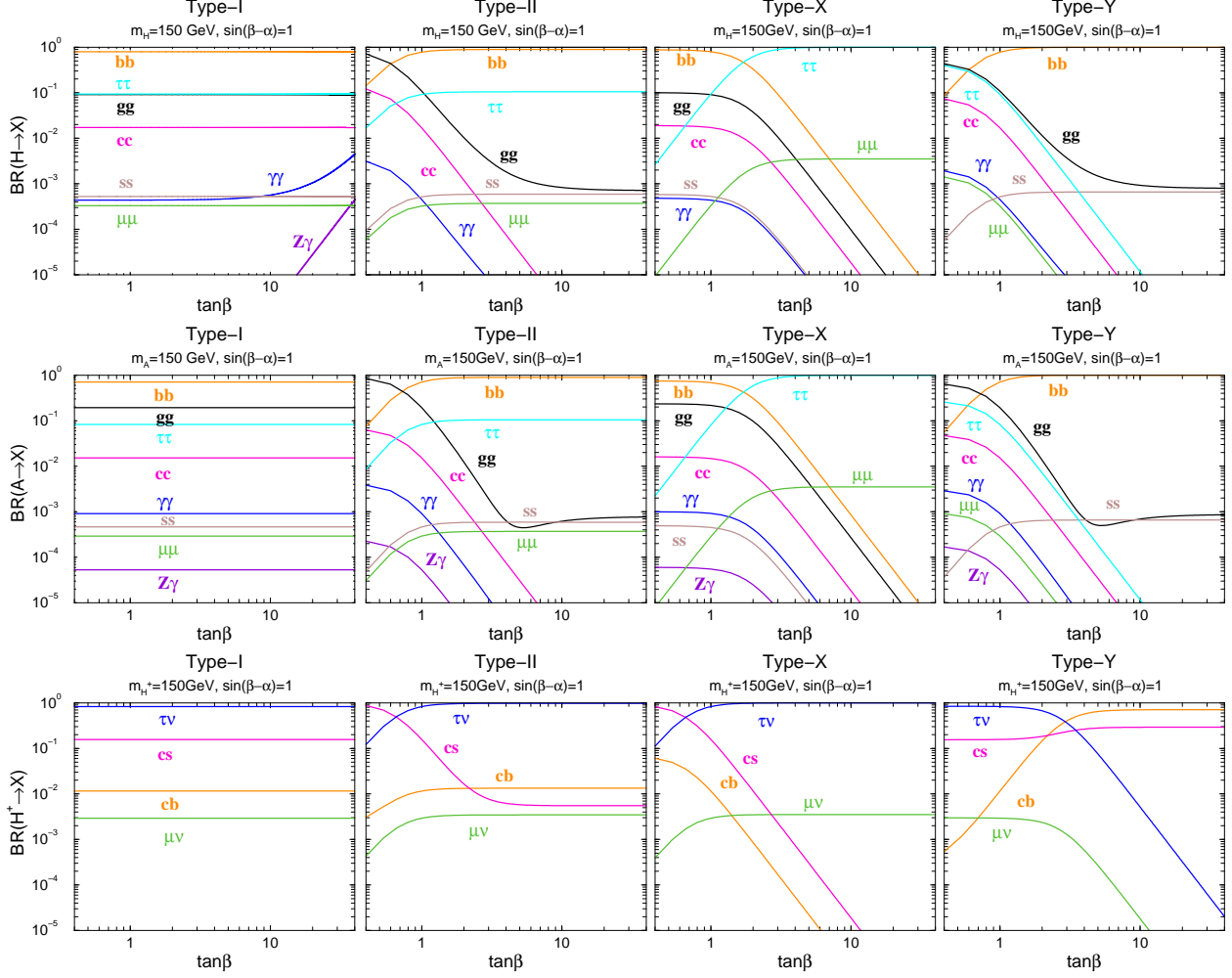


FIG. 2: Decay branching ratios of H , A and H^\pm in the four different types of THDM as a function of $\tan\beta$ for $m_H = m_A = m_{H^\pm} = 150$ GeV and $M = 149$ GeV. The SM-like limit $\sin(\beta - \alpha) = 1$ is taken, where h is the SM-like Higgs boson.

small or negligible. The decay pattern of h is almost the same as that of the SM Higgs boson with the same mass at the leading order except for the loop-induced channels when $\sin(\beta - \alpha) = 1$. In this case, H does not decay into the gauge boson pair at tree level, so it mainly decays into fermion pairs². We note that A and H^\pm do not decay into the gauge boson pair at the tree level for all values of $\sin(\beta - \alpha)$.

The decay patterns are therefore completely different among the different types of Yukawa interactions [11, 12]. For the decays of H and A , we take into account the decay channels

² In the case with a more complicated mass spectrum a heavy Higgs boson can decay into the states which contain lighter Higgs bosons [34].

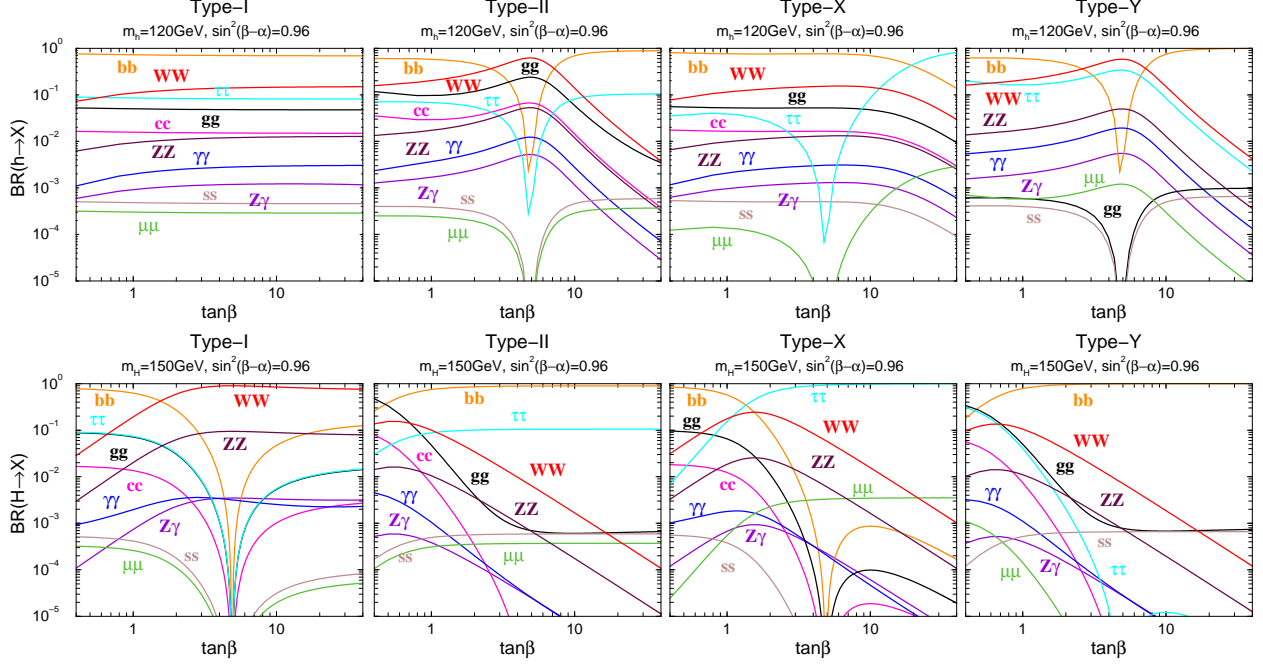


FIG. 3: Decay branching ratios of h and H in the four different types of THDM as a function of $\tan \beta$ for $m_h = 120$ GeV, $m_H = 150$ GeV, $M = 148$ GeV and $\sin^2(\beta - \alpha) = 0.96$.

of $q\bar{q}$, $\ell^+\ell^-$, $(WW^{(*)}, ZZ^{(*)})$ at the tree level, and gg , $\gamma\gamma$, $Z\gamma$ at the leading order, where q represents s , c , b (and t), and ℓ represents μ and τ . Running masses for b , c , and s quarks are fixed as $\overline{m}_b = 3.0$ GeV, $\overline{m}_c = 0.81$ GeV and $\overline{m}_s = 0.046$ GeV, respectively. For the decay of the charged Higgs boson, the modes into tb , cb , cs , $\tau\nu$, and $\mu\nu$ are taken into account as long as they are kinematically allowed. The analytic formulas of each decay rate are given in the Appendix for completeness. They are consistent with the previous results for the type-II THDM [2].

In FIG. 1, the total widths of H , A and H^\pm are shown as a function of the mass of decaying Higgs bosons for several values of $\tan \beta$ in the four different types of Yukawa interactions. We assume $\sin(\beta - \alpha) = 1$ and $m_\Phi = m_H = m_A = m_{H^\pm}$. To keep perturbative unitarity for a wide region of $\tan \beta$, the soft breaking parameter is taken to be $M = m_\Phi - 1$ GeV [30]. The widths strongly depend on the types of Yukawa interactions for each $\tan \beta$ value before and after the threshold of the $t\bar{t}$ (tb) decay mode opens.

In FIG. 2, the decay branching ratios of H , A and H^\pm are shown for $m_\Phi = 150$ GeV, $\sin(\beta - \alpha) = 1$, and $M = m_\Phi - 1$ GeV as a function of $\tan \beta$. In the type-I THDM, the decay of H into a gauge boson pair $\gamma\gamma$ or $Z\gamma$ can increase for large $\tan \beta$ values, because all

the other fermionic decays (including the gg mode) are suppressed but the charged scalar loop contribution to $\gamma\gamma$ and $Z\gamma$ decay modes is not always suppressed for large $\tan\beta$. Such an enhancement of the bosonic decay modes cannot be seen in the decay of A since there is no AH^+H^- coupling. In the type-X THDM, the main decay mode of H and A is $\tau^+\tau^-$ for $\tan\beta \gtrsim 2$, and the leptonic decays $\tau^+\tau^-$ and $\mu^+\mu^-$ become almost 99% and 0.35% for $\tan\beta \gtrsim 10$, while the $b\bar{b}$ (or gg) mode is always the main decay mode in all other cases. In the type-Y THDM, the leptonic decay modes of H and A are rapidly suppressed for large $\tan\beta$ values, and only the branching ratios of $b\bar{b}$ and gg modes are sizable for $\tan\beta \gtrsim 10$. In charged Higgs boson decays with $m_{H^\pm} = 150$ GeV, the decay into $\tau\nu$ is dominant in the type-I THDM, the type-II THDM and the type-X THDMs for $\tan\beta \gtrsim 1$, while hadronic decay modes can also be dominant in the type-Y THDM [11].

In FIG. 3, we show the decay branching ratios of CP-even Higgs bosons, where $m_h = 120$ GeV, $m_\Phi (= m_H = m_A = m_{H^\pm}) = 150$ GeV, $M = 148$ GeV, and $\sin^2(\beta - \alpha) = 0.96$ are taken. Because of the CP-even Higgs boson mixing, the lightest Higgs boson h is no longer purely SM-like. Instead, H can decay into massive gauge bosons via off-shell modes such as WW^* and ZZ^* . Decay patterns of h and H depend on $\tan\beta$ and also on the type of Yukawa interaction. When $\tan\beta \sim 5$, the angle α is nearly zero. In such case coupling constants become small, so that some of fermionic decay modes are suppressed. In order to satisfy the unitarity constraints for the large $\tan\beta$ region, the soft breaking mass scale M must be degenerate to the mass of the decaying bosons [30].

IV. CONSTRAINTS FROM THE CURRENT EXPERIMENTAL DATA ON THDMS

One of the direct signal of the THDM is the discovery of extra Higgs bosons, which have been searched at the LEP and Tevatron [16, 17]. Indirect contributions of Higgs bosons to precisely measurable observables can also be used to constrain Higgs boson parameters. In this section, we summarize these experimental bounds.

A direct mass bound is given from the LEP direct search results as $m_{H^0} \gtrsim 92.8$ GeV for CP-even Higgs bosons and $m_A \gtrsim 93.4$ GeV for CP-odd Higgs bosons in supersymmetric models. The bound for charged Higgs boson has also been set as $m_{H^\pm} \gtrsim 79.3$ GeV [16].

In the THDM, one-loop contributions of scalar loop diagrams to the rho parameter are

expressed as [2]

$$\delta\rho_{\text{THDM}} = \sqrt{2}G_F \frac{1}{(4\pi)^2} \left\{ F_\Delta(m_A^2, m_{H^\pm}^2) - c_{\alpha-\beta}^2 [F_\Delta(m_h^2, m_A^2) - F_\Delta(m_h^2, m_{H^\pm}^2)] - s_{\alpha-\beta}^2 [F_\Delta(m_H^2, m_A^2) - F_\Delta(m_H^2, m_{H^\pm}^2)] \right\}, \quad (7)$$

where $F_\Delta(x, y) = \frac{1}{2}(x+y) - \frac{xy}{x-y} \ln \frac{x}{y}$ with $F_\Delta(x, x) = 0^3$. These quadratic mass contributions can cancel out when Higgs boson masses satisfy the following relation: (i) $m_A \simeq m_{H^\pm}$, (ii) $m_H \simeq m_{H^\pm}$ with $\sin(\beta - \alpha) \simeq 1$, and (iii) $m_h \simeq m_{H^\pm}$ with $\sin(\beta - \alpha) \simeq 0$. These relations correspond to the custodial symmetry invariance [35, 36]. This constraint is independent of the type of Yukawa interaction.

When $m_{H^\pm} \lesssim m_t - m_b$, the top quark can decay into the charged Higgs boson. The decay mode $t \rightarrow H^+ b$ has been studied by using the Tevatron data [37]. The partial decay width is calculated by using the factors ξ_A^f in TABLE II as

$$\Gamma(t \rightarrow H^+ b) = \frac{G_F |V_{tb}|^2}{8\sqrt{2}\pi m_t} \lambda \left(\frac{m_b^2}{m_t^2}, \frac{m_{H^\pm}^2}{m_t^2} \right)^{1/2} \times \left\{ m_t^2 \left[m_t^2 \xi_A^{u2} \left(1 + \frac{m_b^2}{m_t^2} - \frac{m_{H^\pm}^2}{m_t^2} \right) + m_b^2 \xi_A^{d2} \right] + 4m_t^2 m_b^2 \xi_A^u \xi_A^d \right\}, \quad (8)$$

where $\lambda(x, y)$ is defined in Eq. (A5). The higher order corrections can be found in Ref. [38]. The decay branching fraction strongly depends on the type of Yukawa interaction. In the type-I (type-X) THDM, the decay mode can be sizable only for small $\tan\beta$. On the other hand, it can also be substantial for the large $\tan\beta$ region in the type-II (type-Y) THDM since the bottom quark Yukawa coupling receives considerable enhancement. This fact gives a lower bound $1 \lesssim \tan\beta$ for THDMs and an upper bound $\tan\beta \lesssim 60$ for the type-II (type-Y) THDM below $m_{H^\pm} \lesssim 130\text{GeV}$ [37].

It has been known that the charged Higgs boson mass in the type-II THDM is stringently constrained by the precision measurements of the radiative decay of $b \rightarrow s\gamma$ at Belle [39] and BABAR [40] as well as CLEO [41]. The process $b \rightarrow s\gamma$ receives contributions from the W boson loop and the charged Higgs boson loop in the THDM. A notable point is that these two contributions always work constructively in the type-II (type-Y) THDM, while this is

³ There are other (relatively smaller in most of the parameter space) contributions to the rho parameter in the THDM, i.e., those from the diagrams where the gauge boson (as well as Nambu-Goldstone boson) and the Higgs boson are running together in the loop[2]. We have included these effect in our numerical analysis.

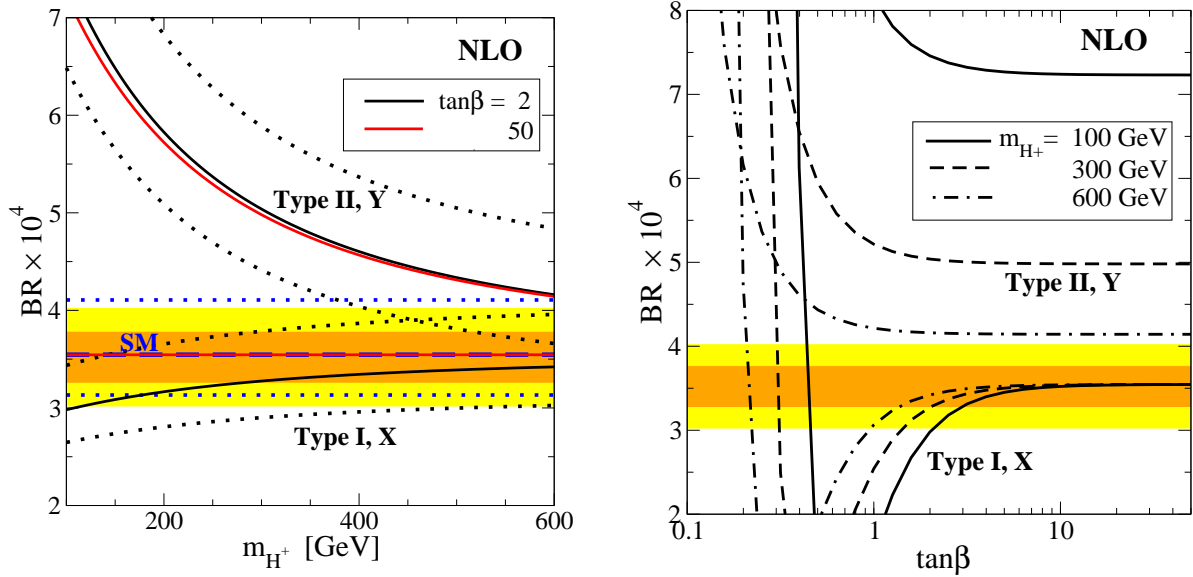


FIG. 4: Predictions of the decay branching ratio for $b \rightarrow s\gamma$ are shown at the NLO approximation as a function of m_{H^\pm} and $\tan\beta$. The dark (light) shaded band represents 1σ (2σ) allowed region of current experimental data. In the left panel, solid (dashed) curves denote the prediction for $\tan\beta = 2$ (50) in various THDMs. In the right panel, solid, dashed and dot-dashed curves are those for $m_{H^\pm} = 100, 300$ and 600 GeV, respectively.

not the case in the type-I (type-X) THDM [11]. In FIG. 4, we show the branching ratio of $B \rightarrow X_s\gamma$ for each type of THDM as a function of m_{H^\pm} (left-panel) and $\tan\beta$ (right-panel), which are evaluated at the next-to-leading order (NLO) following the formulas in Ref. [18]. The SM prediction at the NLO is also shown for comparison. The theoretical uncertainty is about 15%⁴ in the branching ratio (as indicated by dotted curves in FIG. 4), which mainly comes from the pole mass of charm quark $m_c^{\text{pole}} = 1.65 \pm 0.18$ GeV [42]. The experimental bounds of the branching ratio are also indicated, where the current world average value is given by $\mathcal{B}(B \rightarrow X_s\gamma) = (3.52 \pm 0.23 \pm 0.09) \times 10^{-4}$ [43]. It is seen in FIG. 4 that the branching ratio in the type-I (type-X) THDM lies within the 2σ experimental error in all the regions of m_{H^\pm} indicated for $\tan\beta \gtrsim 2$, while that in the type-II (type-Y) THDM is far from the value indicated by the data for a light charged Higgs boson region ($m_{H^\pm} \lesssim 200$ GeV). In the right figure, a cancellation occurs in the type-I (type-X) THDM since there are destructive interferences between the W boson and the H^\pm contributions. It

⁴ In Ref. [18], the theoretical uncertainty is smaller because the value for the error in $m_c^{\text{pole}}/m_b^{\text{pole}}$ is taken to be 7%, which gives main uncertainty in the branching ratio.

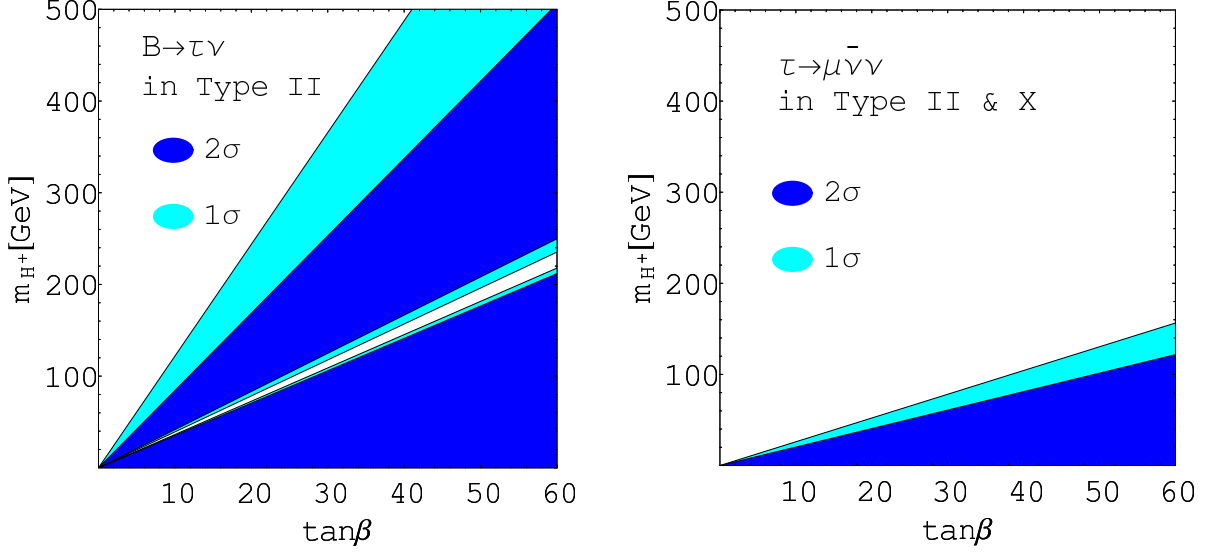


FIG. 5: Bounds from $B \rightarrow \tau\nu$ (left panel) and tau leptonic decay (right panel) on m_{H^\pm} as a function of $\tan\beta$ are shown. The dark (light) shaded region corresponds to the 2σ (1σ) exclusion of these experimental results. In the type-II THDM the wide parameter space is constrained by $B \rightarrow \tau\nu$, while only the tau leptonic decays are important for the type-X THDM.

is emphasized that the charged Higgs boson could be light in the type-I (type-X) THDM under the constraint from $B \rightarrow X_s\gamma$ results. We note that in the MSSM the chargino contribution can compensate the charged Higgs boson contribution [44]. This cancellation weakens the limit on m_{H^\pm} from $b \rightarrow s\gamma$ in the type-II THDM, and allows a light charged Higgs boson as in the type-I (type-X) THDM.

We give some comments on the NNLO analysis, although it is basically out of the scope of this paper. At the NNLO, the branching ratio for $b \rightarrow s\gamma$ has been evaluated in the SM in Ref. [20, 21]. The predicted value at the NNLO is less than that at the NLO approximation in a wide range of renormalization scale. In Ref. [20], the SM branching ratio is $(3.15 \pm 0.23) \times 10^{-4}$, and the lower bound of the m_{H^\pm} , after adding the NLO charged Higgs contribution, is estimated as $m_{H^\pm} \gtrsim 295$ GeV (95% CL) in the type-II (type-Y) THDM [20]⁵. On the other hand, in the type-I (type-X) THDM, although the branching ratio becomes smaller as compared to the NLO evaluation, no serious bound on m_{H^\pm} can be found for $\tan\beta \gtrsim 2$. Therefore, charged Higgs boson mass is not expected to be strongly

⁵ In Ref. [21] the NNLO branching ratio in the SM is calculated as $(2.98 \pm 0.26) \times 10^{-4}$, and the mass bound is a little bit relaxed.

constrained in the type-I (type-X) THDM even at the NNLO, and our main conclusion that the type-I (type-X) THDM is favoured for $m_{H^\pm} \lesssim 200$ GeV based on the NLO analysis should not be changed.

The decay $B \rightarrow \tau \nu$ has been discussed in the type-II THDM [22, 23]. The data for $\mathcal{B}(B^+ \rightarrow \tau^+ \nu_\tau) = (1.4 \pm 0.4) \times 10^{-4}$ are obtained at the B factories [42, 45]. The decay branching ratio can be written as [22, 46]

$$\frac{\mathcal{B}(B^+ \rightarrow \tau^+ \nu_\tau)_{\text{THDM}}}{\mathcal{B}(B^+ \rightarrow \tau^+ \nu_\tau)_{\text{SM}}} \simeq \left(1 - \frac{m_B^2}{m_{H^\pm}^2} \xi_A^d \xi_A^\ell\right)^2. \quad (9)$$

In FIG. 5, the allowed region from the $B \rightarrow \tau \nu$ results is shown in the type-II THDM. The dark (light) shaded region denotes the 2σ (1σ) exclusion from the $B \rightarrow \tau \nu$ measurements. The process is important only in the type-II THDM with large $\tan \beta$ values. The other types of Yukawa interactions do not receive constraints from this process.

The rate for the leptonic decay of the tau lepton $\tau \rightarrow \mu \bar{\nu} \nu$ can be deviated from the SM value by the presence of a light charged Higgs boson [24]. The partial decay rate is approximately expressed as [22]

$$\frac{\Gamma_{\tau \rightarrow \mu \bar{\nu} \nu}^{\text{THDM}}}{\Gamma_{\tau \rightarrow \mu \bar{\nu} \nu}^{\text{SM}}} \simeq 1 - \frac{2m_\mu^2}{m_{H^\pm}^2} \xi_A^{\ell^2} \kappa \left(\frac{m_\mu^2}{m_\tau^2} \right) + \frac{m_\mu^2 m_\tau^2}{4m_{H^\pm}^4} \xi_A^{\ell^4}, \quad (10)$$

where $\kappa(x) = g(x)/f(x)$ is defined by $f(x) = 1 - 8x - 12x^2 \ln x + 8x^3 - x^4$, and $g(x) = 1 + 9x - 9x^2 - x^3 + 6x(1+x) \ln x$. In the type-II (type-X) THDM, the leptonic Yukawa interaction can be enhanced in the large $\tan \beta$ region. Hence, both the models are weakly constrained by tau decay data, as in FIG. 5.

The precision measurement for the muon anomalous magnetic moment can give mass bound on the Higgs boson in the SM [25]. This constraint can be applied for more general interaction, including THDMs [26]. At the one-loop level, the contribution is given by

$$\delta a_\mu^{1\text{-loop}} \simeq \frac{G_F m_\mu^4}{4\pi^2 \sqrt{2}} \left[\sum_{\phi^0=h,H} \frac{\xi_{\phi^0}^{\ell^2}}{m_{\phi^0}^2} \left(\ln \frac{m_{\phi^0}^2}{m_\mu^2} - \frac{7}{6} \right) + \frac{\xi_A^{\ell^2}}{m_A^2} \left(-\ln \frac{m_A^2}{m_\mu^2} + \frac{11}{6} \right) - \frac{\xi_A^{\ell^2}}{6m_{H^\pm}^2} \right]. \quad (11)$$

This process is also purely leptonic and only gives milder bounds on the Higgs boson masses for very large $\tan \beta$ values in the type-II (type-X) THDM. It gives no effective bound on the type-I (type-Y) THDM. It is also known that the two-loop (Barr-Zee type) diagram can significantly affect a_μ [47, 48]. The contribution can be large because of the enhancement

factors of m_f^2/m_μ^2 and also of the mixing factors ξ_ϕ^f as [48]

$$\delta a_\mu^{\text{BZ}} \simeq \frac{N_c^f Q_f^2 G_F \alpha m_\mu^2}{4\pi^3 v^2} \left[- \sum_{\phi^0=h,H} \xi_{\phi^0}^\ell \xi_{\phi^0}^f f\left(\frac{m_f^2}{m_{\phi^0}^2}\right) + \xi_A^\ell \xi_A^f g\left(\frac{m_f^2}{m_A^2}\right) \right], \quad (12)$$

where

$$f(z) = \frac{z}{2} \int_0^1 dx \frac{1-2x(1-x)}{x(1-x)-z} \ln \frac{x(1-x)}{z}, \quad (13)$$

$$g(z) = \frac{z}{2} \int_0^1 dx \frac{1}{x(1-x)-z} \ln \frac{x(1-x)}{z}. \quad (14)$$

The contribution from this kind of diagram is only important for large $\tan\beta$ values with smaller Higgs boson masses in the type-II THDM. For the other types of THDM, it would give a much less effective bound on the parameter space.

V. COLLIDER SIGNALS IN THE TYPE-X THDM AT THE LHC AND THE ILC

We discuss the collider phenomenology of the models at the LHC and the ILC. There have already been many studies on the production and decays of the Higgs bosons in the type-II THDM, especially in the context of the MSSM, while the phenomenology of the other types of THDMs has not yet been studied sufficiently. Recently, the type-X THDM has been introduced in the model to explain phenomena such as neutrino masses, dark matter, and baryogenesis at the TeV scale [7]. We therefore concentrate on the collider signals in the type-X THDM, and discuss how we can distinguish the model from the type-II THDM (the MSSM), mainly in scenarios with a light charged Higgs boson ($100 \text{ GeV} \lesssim m_{H^\pm} \lesssim 300 \text{ GeV}$). (Such a light charged Higgs boson is severely constrained by the $b \rightarrow s\gamma$ result in the non-supersymmetric type-II THDM and the type-Y THDM, while it can be allowed in the MSSM and the type-X (type-I) THDM.) As we are interested in the differences in the types of the Yukawa interactions, we focus here on the case of $m_{H^\pm} \simeq m_A \simeq m_H$ with $\sin(\beta - \alpha) \simeq 1$ for definiteness.

A. Charged Higgs boson searches at the LHC

A light charged Higgs boson with $m_{H^\pm} \lesssim m_t - m_b$ can be produced in the decay of top quarks at the LHC. The discovery potential for the charged Higgs boson via the $t\bar{t}$

production has been studied in the MSSM [37]. Assuming an integrated luminosity of 30 fb⁻¹, the expected signal significance of the event $t\bar{t} \rightarrow H^\pm W^\mp b\bar{b} \rightarrow \ell\nu\tau\nu_\tau b\bar{b}$ is greater than 5σ for $m_{H^\pm} \lesssim 130$ GeV for $\tan\beta \lesssim 2$ and $\tan\beta \gtrsim 20$ [37]. The same analysis can also be applied for the type-X THDM, in which a similar number of H^\pm can be produced when $\tan\beta \sim \mathcal{O}(1)$. The main decay mode ($\tau\nu$) is common in the type-II THDM and the type-X THDM, except for very low $\tan\beta$ values. Thus, searching for neutral Higgs bosons is important to distinguish the difference in the types of Yukawa interactions.

For $m_{H^\pm} \gtrsim m_t$, charged Higgs bosons can be produced in $q\bar{q}/gg \rightarrow t\bar{b}H^-$, $gb \rightarrow tH^-$ [49, 50], $gg (q\bar{q}) \rightarrow H^+H^-$ [51, 52] and $gg (b\bar{b}) \rightarrow H^\pm W^\mp$ [53]. These processes, except for the H^+H^- production, are via the Yukawa coupling of $t\bar{b}H^-$, so that the cross sections are significant for $\tan\beta \sim \mathcal{O}(1)$ or $\tan\beta \gtrsim 10$ –20 in the type-II THDM and only for $\tan\beta \sim \mathcal{O}(1)$ in the type-X THDM. The type of Yukawa interaction in the THDM can then be discriminated by measuring the difference in decay branching ratios of H^\pm . In the type-II THDM H^\pm mainly decay into tb , while $\tau\nu$ is dominant for $\tan\beta \gtrsim 10$ in the type-X THDM.

B. Neutral Higgs boson (A and H) production at the LHC

At the LHC, the type of the Yukawa interaction may be determined in the search for neutral Higgs bosons through the direct production via gluon fusion $gg \rightarrow A/H$ [52, 54], vector boson fusion $V^*V^* \rightarrow H$, $V = W, Z$ [55, 56], and also via associated production $pp \rightarrow b\bar{b}A (b\bar{b}H)$ [57, 58]. The production process $pp \rightarrow t\bar{t}A (t\bar{t}H)$ [50, 58, 59] can also be useful for $\tan\beta \sim 1$. We discuss the possibility of discriminating the type of the Yukawa interaction by using the production and decay processes of A and H for $\sin(\beta - \alpha) = 1$. Additional neutral Higgs bosons A and H are directly produced by the gluon fusion mechanism at the one-loop level. When $\sin(\beta - \alpha) \simeq 1$, the production rate can be significant due to the top quark loop contribution for $\tan\beta \sim 1$ and, in the MSSM (the type-II THDM), also for large $\tan\beta$ via the bottom quark loop contributions [52]. Notice that there is no rate of $V^*V^* \rightarrow A$ because there is no VVA coupling, and that the production of H from the vector boson fusion $V^*V^* \rightarrow H$ is relatively unimportant when $\sin(\beta - \alpha) \simeq 1$. The associated production process $pp \rightarrow b\bar{b}A (b\bar{b}H)$ can be significant for large $\tan\beta$ values in the MSSM (the type-II THDM) [57].

In the MSSM (the type-II THDM), the produced A and H in these processes decay mainly into $b\bar{b}$ when $\sin(\beta - \alpha) \simeq 1$, which would be challenging to detect because of huge QCD backgrounds. Instead, the decays into a lepton pair $\tau^+\tau^-$ ($\mu^+\mu^-$) would be useful for searches of A (and H). However, the decay branching ratios of $A \rightarrow \tau^+\tau^-$ ($\mu^+\mu^-$) are less than 0.1 (0.0004). A simulation study [60] shows that the Higgs boson search via the associate production $b\bar{b}A$ ($b\bar{b}H$) is better than that via the direct production from gluon fusion to see both $\tau^+\tau^-$ and $\mu^+\mu^-$ modes, especially in the large $\tan\beta$ area. The largest background is the Drell-Yan process from $\gamma^*/Z^* \rightarrow \tau^+\tau^-$ (and $\mu^+\mu^-$). The other ones, such as $t\bar{t}$, $b\bar{b}$ and $W + jet$, also contribute to the backgrounds. The rate of the $\tau^+\tau^-$ process from the signal is much larger than that of the $\mu^+\mu^-$ one. However, the resolution for tau leptons is much broader than that for muons, so that for relatively small m_A (m_H) the $\mu^+\mu^-$ mode can be more useful than the $\tau^+\tau^-$ mode [61].

In the type-X THDM, signals from the associate production $pp \rightarrow b\bar{b}A$ are very difficult to detect. The production cross section is at most 150 fb for $m_A = 150$ GeV at $\tan\beta = 1$ [60], where the branching ratio $A \rightarrow \tau^+\tau^-$ and $A \rightarrow \mu^+\mu^-$ are small, and the produced signals are less for larger values of $\tan\beta$. On the other hand, the direct production from $gg \rightarrow A/H$ can be used to see the signal. The cross sections are significant for $\tan\beta \sim 1$, and they decrease for larger values of $\tan\beta$ by a factor of $1/\tan^2\beta$. However, the branching ratios of $A/H \rightarrow \tau^+\tau^-$ dominate over those of $A/H \rightarrow b\bar{b}$ for $\tan\beta \gtrsim 2$ and become almost 100% for $\tan\beta \gtrsim 4$ (see FIG. 2). Therefore, large significances can be expected around $\tan\beta \sim 2$ in the type-X THDM.

In FIG. 6, we show the expected signal significance of the direct production $pp(gg) \rightarrow A/H \rightarrow \tau^+\tau^-$ in the type-X THDM and the MSSM at the LHC, assuming an integrated luminosity of 30 fb^{-1} . The mass of the CP-odd Higgs boson m_A is taken to be 150 GeV in both models, while m_H is 150 GeV for the results of the type-X THDM and that in the MSSM is deduced using the MSSM mass relation. For the detailed analysis of background simulation, we employed the one shown in the ATLAS TDR [60]. The basic cuts, such as the high p_T cut and the standard $A/H \rightarrow \tau^+\tau^-$ reconstruction, are assumed [60]. We can see that, for the search of the direct production, the signal significance in the type-X THDM can be larger than that in the MSSM for $\tan\beta \lesssim 5$. In particular, the signal in the type-X THDM can be expected to be detectable ($S/\sqrt{B} > 5$) when $\tan\beta \sim 2$ for the luminosity of 30 fb^{-1} . For smaller values of m_A (m_H), the production cross section becomes large so

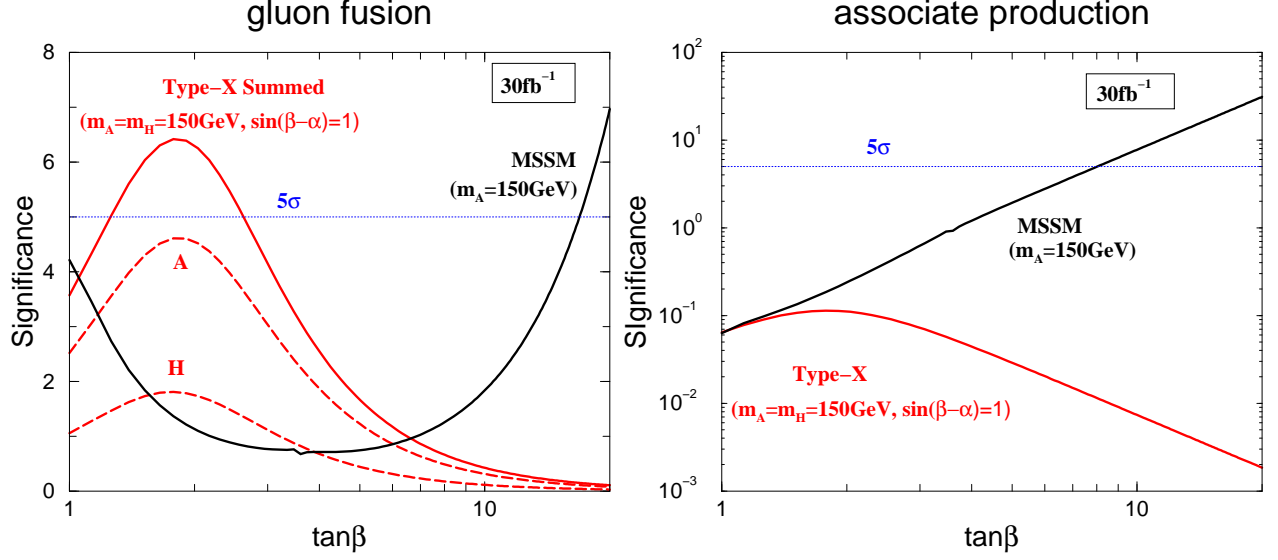


FIG. 6: Signal significance (S/\sqrt{B}) for gluon fusion $gg \rightarrow A/H$ (left panel) and the associated production $pp \rightarrow b\bar{b}A$ ($b\bar{b}H$) (right panel) with the $\tau^+\tau^-$ final state in the type-X THDM and the MSSM. In both figures, the dashed and the solid curves represents the expected values of signal significance for A/H and summed over A and H . The red (thin) curves denote the significance in the type-X THDM, while the black (thick) solid curves denote that in the MSSM.

that the signal rate is more significant, but the separation from the Drell-Yan background becomes more difficult because the resolution of the tau lepton is broad. Therefore, the significance becomes worse for $m_A(m_H) \lesssim 130$ GeV.

When A and H are lighter than 130 GeV, the $\mu^+\mu^-$ mode can be more useful than the $\tau^+\tau^-$ mode. The resolution of muons is much better than that of tau leptons, so that the invariant mass cut is very effective in reducing the background from $\gamma^*/Z^* \rightarrow \mu^+\mu^-$. The feasibility of the process $gg \rightarrow A/H \rightarrow \mu^+\mu^-$ has been studied in the SM and the MSSM in Refs. [60, 61]. We evaluate the signal significances of $gg \rightarrow A/H \rightarrow \mu^+\mu^-$ in the type-X THDM by using the result in Ref. [61]. In TABLE III, we list the results of the significance in the SM and the type-X THDM. According to Tao Han's paper, the basic kinematic cuts of $p_T > 20$ GeV, $|\eta| < 2.5$ and the invariant mass cuts as $m_{A/H} - 2.24$ GeV $< M_{\mu\mu} < m_{A/H} + 2.24$ GeV are used ⁶. The integrated luminosity is assumed to be 300

⁶ This choice for the invariant mass cut is rather severe; i.e., it requires the precise determination of m_A and m_H . If the range of the invariant mass cut is taken to be double, roughly speaking, background events also become double. This would suppress the signal significance in TABLE III by a factor of $\sim 1/\sqrt{2}$.

m_ϕ [GeV]	SM (H_{SM})	MSSM(A)	Type-X (H)	Type-X (A)	Type-X(Sum) ($m_A \simeq m_H$)
115	2.41	1.31	4.31	12.0	16.3
120	2.51	1.49	4.89	13.4	18.3
130	2.25	1.81	5.78	15.6	21.4
140	1.61	2.11	6.60	17.5	24.1

TABLE III: Expected signal significances for $gg \rightarrow \phi \rightarrow \mu^+\mu^-$ ($\phi = H_{\text{SM}}, H, A$) in the SM, the MSSM, and the type-X THDM. For the results in the MSSM $\tan\beta = 2$ is taken, and for that in the type-X THDM $\tan\beta = 2$ and $\sin(\beta - \alpha) = 1$ are taken. The integrated luminosity is assumed to be 300 fb^{-1} .

fb^{-1} . For the results in the type-X THDM, $\tan\beta = 2$ and $\sin(\beta - \alpha) = 1$ are taken. The results show that the significance can be substantial for $m_A \gtrsim 115 \text{ GeV}$ when $\tan\beta = 2$. For smaller masses of the extra Higgs bosons, the cross section for the signal processes can be larger, but the invariant mass cut becomes less effective in the reduction of the Drell-Yan background because of the smaller mass difference between m_Z and m_A ; hence, the signal significance becomes worse. The $\tan\beta$ dependence in the signal significance for the muon final states is also shown in FIG. 7. The shape of the curves is similar to that for the tau lepton final state in FIG 6.

In summary, we would be able to distinguish the type-X THDM from the MSSM by measuring the leptonic decays of the additional Higgs bosons produced via the direct search processes $gg \rightarrow A/H \rightarrow \tau^+\tau^-$ ($\mu^+\mu^-$) and the associated processes $pp \rightarrow b\bar{b}A$ ($b\bar{b}H$). First, if a light scalar boson is found via $gg \rightarrow h \rightarrow \gamma\gamma$ or $W^+W^- \rightarrow h \rightarrow \gamma\gamma$ ($\tau^+\tau^-$) and if the event number is consistent with the prediction in the SM, then we know that the scalar boson is of the SM or at least SM-like: in the THDM framework this means $\sin(\beta - \alpha) \simeq 1$, assuming that it is the lightest one. Second, under the situation above, when the associated production $pp \rightarrow b\bar{b}A$ ($b\bar{b}H$) is detected at a different invariant mass than the mass of the SM-like one and no $gg \rightarrow A/H \rightarrow \tau^+\tau^-$ ($\mu^+\mu^-$) is found at that point, we would be able to identify the MSSM Higgs sector (or the type-II THDM) with high $\tan\beta$ values. On the other hand, the type-X THDM with low $\tan\beta$ would be identified by finding the signal from the gluon fusion process without that from the $b\bar{b}\tau^+\tau^-$. If signals from the direct production processes are found but the number is not sufficient, then the value of $\tan\beta$ would be around

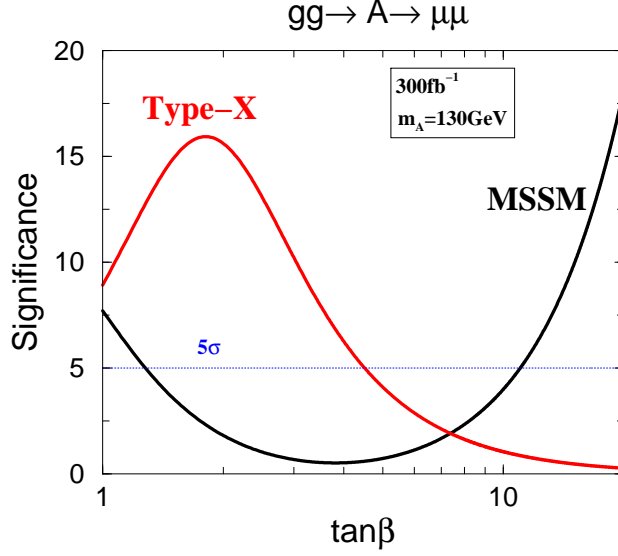


FIG. 7: Signal significance (S/\sqrt{B}) for the $\mu^+\mu^-$ final state from gluon fusion $gg \rightarrow A$ in the type-X THDM and the MSSM. The red (thin) curves denote significance in the type-X THDM, while the black (thick) solid curves denote that in the MSSM.

6–10 ($m_t \cot \beta \sim m_b \tan \beta$), where the rates in the MSSM and the type-X THDM are similar. In this case, it would be difficult to distinguish these models from the above processes. As we discussed in the next subsection, Higgs pair production processes $pp \rightarrow AH^\pm, HH^\pm$, and AH can be useful to measure the Yukawa interaction through branching fractions, because these production mechanism do not depend on $\tan \beta$ in such a situation.

We have concentrated on $\sin(\beta - \alpha) \simeq 1$ in this analysis because the parameter is motivated in Ref. [7]. Here we comment on the situation without the condition $\sin(\beta - \alpha) = 1$. If $\sin(\beta - \alpha)$ is not close to unity, our conclusion can be modified. The production cross sections of $gg \rightarrow A/H$ and $pp \rightarrow b\bar{b}A(b\bar{b}H)$ can be enhanced in the type-X THDM for $\tan \beta \gtrsim 1$ since the factor $(\sin \alpha / \sin \beta)$ of quark-Higgs couplings can be large in a specific region of the parameter space. The signal of the CP odd Higgs boson A can then be significant. On the other hand, the CP even Higgs boson H can decay into WW^* when $\sin(\beta - \alpha)$ is not unity. This would reduce leptonic branching fractions. The signal can be enhanced only for large $\tan \beta$ regions because leptonic decays are significant only for such a parameter space. We also note that H can be produced significantly by the vector boson fusion mechanism in a mixing case.

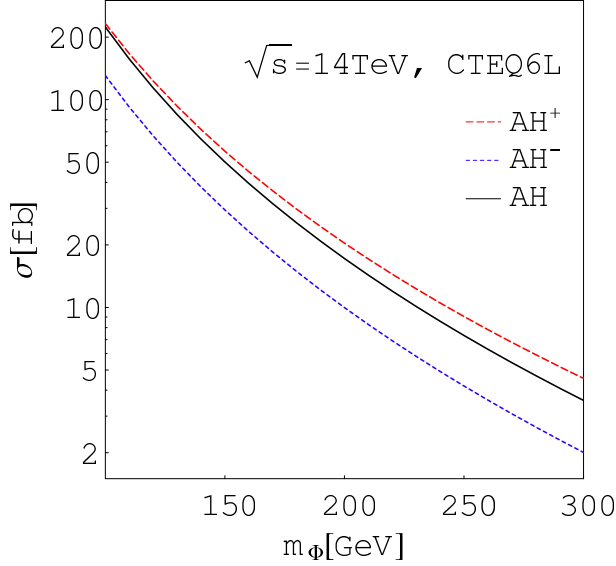


FIG. 8: Production cross sections of $pp \rightarrow AH^\pm$ and AH are shown at the leading order as a function of scalar boson masses in the THDM where $m_\Phi = m_H = m_A = m_{H^\pm}$ are chosen. The long-dashed, dashed and solid curves denote the pair production of AH^+ , AH^- and AH , respectively. The cross section of $pp \rightarrow HH^\pm$ is the same as those of $pp \rightarrow AH^\pm$ when $\sin(\beta - \alpha) = 1$.

C. Pair production of extra Higgs bosons at the LHC

The types of the Yukawa interactions can be studied using the process of $q\bar{q}' \rightarrow W^{\pm*} \rightarrow AH^\pm$ (HH^\pm) [52, 62, 63, 64, 65] and $q\bar{q} \rightarrow Z^* \rightarrow AH$ [52], unless the extra Higgs bosons H , A and/or H^\pm are too heavy ⁷. Hadronic cross sections for these processes are shown at the leading order in FIG. 8 as a function of the mass of the produced scalar boson Φ , where $m_\Phi = m_H = m_A = m_{H^\pm}$. Expected rates of AH^\pm (sum) and AH are about 143 fb and 85 fb for $m_{H^\pm} = 130$ GeV and about 85 fb and 50 fb for $m_{H^\pm} = 150$ GeV, respectively. The NLO QCD corrections are expected to enhance these rates typically by about 20% [62, 64]. The production rates are common in all the types of THDMs, because the cross sections are determined only by the masses of the produced scalar bosons. Therefore, they are very sensitive to the difference in the decay branching ratios of the produced Higgs bosons. In the MSSM, the $b\bar{b}\tau^\pm\nu$ ($b\bar{b}\tau^+\tau^-$) events can be the main signal of the AH^\pm and HH^\pm (AH) processes, while in the type-X THDM ($\tan\beta \gtrsim 2$), $\tau^+\tau^-\tau^\pm\nu$ ($\tau^+\tau^-\tau^+\tau^-$) would be the main

⁷ When the mixing between h and H is large, the hH^\pm production can also be important [65].

signal events.

In the MSSM, the parton level background analysis for the AH^\pm (HH^\pm) production process has been performed in Ref. [64, 65] by using the $b\bar{b}\tau\nu$ final state. The largest background comes from $q\bar{q}' \rightarrow Wg^* \rightarrow Wb\bar{b}$, which can be reduced by basic kinematic cuts and the invariant mass cut of $b\bar{b}$, as well as by the kinematic cut to select hard hadrons from the parent τ^\pm from H^\pm . It has been shown that a sufficient signal significance can be obtained for smaller masses of Higgs bosons [64].

In the type-X THDM, the produced AH^\pm (HH^\pm) and AH pairs can be studied via the leptonic decays. Hence these channels can be useful to discriminate the type-X THDM from the MSSM. Assuming an integrated luminosity of 300 fb^{-1} , 8.6×10^4 and 5.1×10^4 of the signal events are produced from both AH^\pm and HH^\pm production for $m_\Phi = 130 \text{ GeV}$ and 150 GeV , respectively, where $m_\Phi = m_H = m_A = m_{H^\pm}$. A and H (H^\pm) decay into $\tau^+\tau^-$ ($\tau\nu$) by more than 95% and 95% (99%) for $\tan\beta \gtrsim 4$, respectively. The purely leptonic signal would have an advantage in the signal to background ratio because the background from the intermediate state $q\bar{q}' \rightarrow Wg^*$ would be negligible. For $\tan\beta = 7$, the produced AH^\pm and HH^\pm pairs almost all (more than 99%) go to $\tau^+\tau^-\tau\nu$ final states. The numbers of signal and background are summarized in TABLE IV. The signal to background ratio for $\tau^+\tau^-\tau\nu$ final state is not so small $\mathcal{O}(0.1\text{--}1)$, before cuts⁸. The backgrounds are expected to be reduced by using high- p_T cuts, hard hadrons from the parent tau leptons from H^\pm , and invariant mass cuts for $\tau^+\tau^-$ from A and H , in addition to the basic cuts. However, the signal significance strongly depend on the rate of miss identification of hadrons as tau leptons, so that a realistic simulation is necessary.

We also would be able to use the $\mu^+\mu^-\tau^+\nu$ events to identify the AH^+ and HH^+ production in the type-X THDM, by using the much better resolution of $\mu^+\mu^-$ in performing the invariant mass cuts. For 300 fb^{-1} , the AH^+ and HH^+ process can produce about $\mathcal{O}(100)$ of $\mu^+\mu^-\tau^+\nu$ events for $m_A = m_H = 130 \text{ GeV}$. The number of background events is about 3.1×10^5 of $\mu^+\mu^-\tau^+\nu$ from ZW^\pm production. Signals and background for $\mu^+\mu^-\tau^+\nu$ events are also summarized in TABLE IV. The background can be expected to be reduced by imposing a selection of the events around the invariant mass of $m_A \sim M_{\mu\mu}$ and the high p_T

⁸ The γW^\pm production may give a much larger cross section for background events. It may also be reduced considerably by kinematic cuts.

	$AH^\pm, HH^\pm(m_\Phi = 130 \text{ GeV})$	$AH^\pm, HH^\pm(m_\Phi = 150 \text{ GeV})$	ZW^\pm
$\tau^+\tau^-\tau\nu$	8.4×10^4	5.0×10^4	3.2×10^4
$\mu^+\mu^-\tau\nu$	3.0×10^2	1.8×10^2	3.1×10^4

TABLE IV: Events for the $\tau^+\tau^-\tau\nu$ and $\mu^+\mu^-\tau\nu$ final states from the Higgs boson pair production and ZW^\pm background. The signal events are summed over AH^\pm and HH^\pm . The integrated luminosity is taken to be 300 fb^{-1} . Values for the decay branching ratios are taken to be $\mathcal{B}(A/H \rightarrow \tau^+\tau^-) = 0.99$, $\mathcal{B}(A/H \rightarrow \mu^+\mu^-) = 0.0035$, and $\mathcal{B}(H^\pm \rightarrow \tau\nu) = 0.99$, which correspond to the values for $\tan\beta \gtrsim 7$. The cross section of $pp \rightarrow ZW^\pm$ is evaluated as $\sigma_{ZW} = 27.7 \text{ pb}$ by CalcHEP [66].

	$AH(m_\Phi = 130 \text{ GeV})$	$AH(m_\Phi = 150 \text{ GeV})$	ZZ
$\tau^+\tau^-\tau^+\tau^-$	2.5×10^5	1.5×10^5	3.6×10^3
$\tau^+\tau^-\mu^+\mu^-$	1.8×10^2	1.0×10^2	7.1×10^3

TABLE V: Events for the $\tau^+\tau^-\tau^+\tau^-$ and $\tau^+\tau^-\mu^+\mu^-$ final states from the Higgs boson pair production and ZZ background. The integrated luminosity is taken to be 300 fb^{-1} . The cross section of $pp \rightarrow ZZ$ is evaluated as $\sigma_{ZZ} = 10.5 \text{ pb}$ by CalcHEP [66].

cuts. Hard hadrons from the decay of τ 's from H^+ can also be used to reduce the background. In the MSSM, much smaller signals are expected, so that this process can be a useful probe of the type-X THDM.

In a similar way, we may use AH production [52] to identify the type-X THDM. For the $\tau^+\tau^-\tau^+\tau^-$ decay mode, the signal is evaluated approximately as 2.5×10^4 events, assuming 300 fb^{-1} for $m_A = m_H = 130 \text{ GeV}$ and $\tan\beta = 7$. The main background may come from the $q\bar{q} \rightarrow ZZ$ process. We also consider the $\mu^+\mu^-\tau^+\tau^-$ decay mode. The number of signal event is $\mathcal{O}(100)$ for an integrated luminosity 300 fb^{-1} . The numbers of signal and background event are listed in TABLE V. It would be valuable to use the detailed background simulation.

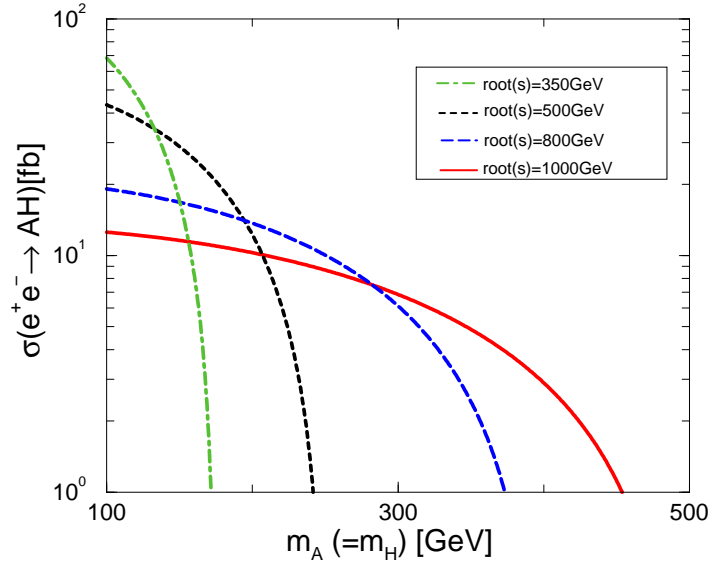


FIG. 9: The production cross section of $e^+e^- \rightarrow AH$ is shown as a function of the Higgs boson mass. The dot-dashed, dashed, long-dashed, and solid curves correspond to $\sqrt{s} = 350, 500, 800$, and 1000 GeV, respectively.

D. Pair production of extra Higgs bosons at the ILC

At the ILC, we would be able to test the types of the Yukawa interactions via the pair production of the additional Higgs bosons $e^+e^- \rightarrow AH$ [52, 67]. In Fig. 9, the production cross section is shown for $\sqrt{s} = 350, 500, 800$, and 1000 GeV as a function of m_A assuming $m_A = m_H$ in the THDM. The production rate is determined only by m_A , and m_H at the leading order, and is independent of $\tan\beta$. (In the MSSM, it depends indirectly on $\tan\beta$ via the mass spectrum.) The signal of the type-X THDM can be identified by searching for the events of $\tau^+\tau^-\tau^+\tau^-$ and $\mu^+\mu^-\tau^+\tau^-$. When $\sqrt{s} = 500$ GeV, assuming an integrated luminosity of 500 fb^{-1} , the event number is estimated as 1.6×10^4 (1.8×10^2) in the type-X (type-II) THDM for $\tau^+\tau^-\tau^+\tau^-$, and 1.1×10^2 (0.6) for $\mu^+\mu^-\tau^+\tau^-$ assuming $m_H = m_A = m_{H^\pm} = 130$ GeV, $\sin(\beta - \alpha) = 1$ and $\tan\beta = 10$. This number does not change much for $\tan\beta \gtrsim 3$. The main background comes from the Z pair production, whose rate is about $4 \times 10^2 \text{ fb}$. The event numbers from the background are then 2.3×10^2 for $\tau^+\tau^-\tau^+\tau^-$ and 4.6×10^2 for $\mu^+\mu^-\tau^+\tau^-$. Therefore, the signal should be easily detected in the type-X THDM, by which we would be able to distinguish the type-X from the type-II (the MSSM).

The detailed measurement of the masses of additional Higgs bosons and Yukawa coupling constants will make it possible to determine the scenario of physics beyond the SM through

the Higgs physics.

VI. DISCUSSIONS AND CONCLUSIONS

We have discussed the phenomenology of the four possible types of Yukawa interactions in the THDM with softly broken discrete Z_2 symmetry. Although the particle contents are the same in these models, their phenomenologies are completely different from each other. In some new physics models, two Higgs doublets (plus singlets) are introduced with a definite type of Yukawa interaction. Therefore, when additional Higgs bosons are discovered, we may be able to distinguish new physics models via the differences between the types of Yukawa interactions.

The differences between the types of the Yukawa interactions largely affect the decay of the Higgs bosons. We have evaluated the decay branching ratios in each type of THDM. We have then summarized the current experimental bounds on the models from the data of $b \rightarrow s\gamma$, $B \rightarrow \tau\nu$, $\tau \rightarrow \mu\bar{\nu}\nu$ and measurements of muon anomalous magnetic moment. The charged Higgs boson mass can be light ($m_{H^\pm} \lesssim m_t$) in the type-I and type-X THDMs under these experimental limits. Such a light charged Higgs boson is also possible in the MSSM.

We have discussed the collider phenomenology of the THDMs. For definiteness, we have concentrated on phenomenological differences between the MSSM Higgs sector and the type-X THDM in the case of a light charged Higgs boson. The type-X Yukawa interaction is used in TeV-scale models for neutrino masses, dark matter, and baryon asymmetry. At the LHC, the type-X THDM can be discriminated from the MSSM by searching for the production and decays of the extra Higgs bosons A , H , and H^\pm , such as $gg \rightarrow A/H \rightarrow \ell^+\ell^-$, $pp \rightarrow b\bar{b}A$ ($b\bar{b}H$) $\rightarrow b\bar{b}\ell^+\ell^-$, where ℓ is τ or μ when $\sin(\beta-\alpha) \simeq 1$. We also discussed the pair production processes $pp \rightarrow AH^\pm$, HH^\pm , and AH to test the type-X THDM. These processes would provide distinctive four lepton final states $\ell^+\ell^-\tau^\pm\nu$ and $\ell^+\ell^-\tau^+\tau^-$ in the type-X THDM, while the MSSM Higgs sector can be tested by $b\bar{b}\tau^\pm\nu$ and $b\bar{b}\tau^+\tau^-$. Although the realistic simulation study is necessary, the type-X THDM can be identified at the LHC with an integrated luminosity of 300 fb^{-1} . At the ILC, the type-X THDM is expected to be studied very well by the pair production $e^+e^- \rightarrow AH$. The signal should be four leptons ($\ell^+\ell^-\tau^+\tau^-$).

We have discussed phenomenological discrimination of the types of Yukawa interactions in the THDM at future experiments. In particular, we have mainly discussed the separation

at the LHC and the ILC between the MSSM Higgs sector and the type-X THDM in the relatively light charged Higgs boson scenario. By extending this study to include other various cases, we can expect that the types of the Yukawa interactions in extended Higgs models can be completely determined at current and future collider experiments. Such information may be useful to select a true model from many proposed new physics models at TeV scales.

Acknowledgments

We would like to thank Andrew Akeroyd, Yasuhiro Okada, Kaoru Hagiwara, and Jun-ichi Kanzaki for useful comments. The work of S. K. was supported in part by Japan Society for Promotion of Science (JSPS), No. 18034004.

Note added:

After this paper was completed, Refs. [68, 69, 70] appeared in which similar Yukawa interaction is discussed in a different context.

APPENDIX A: HIGGS BOSON DECAY RATES IN THDMS

In the THDM, the partial decay widths of Higgs bosons decaying into a fermion pair are computed at the leading order as

$$\Gamma(\varphi \rightarrow q\bar{q}) = N_C \frac{G_F m_\varphi m_q^2}{4\sqrt{2}\pi} \xi_\varphi^{q^2} \times \begin{cases} \beta_q^3 & \text{for } \varphi = h, H \\ \beta_q & \text{for } \varphi = A \end{cases}, \quad (\text{A1})$$

$$\Gamma(\varphi \rightarrow \ell^+ \ell^-) = \frac{G_F m_\varphi m_\ell^2}{4\sqrt{2}\pi} \xi_\varphi^{\ell^2} \times \begin{cases} \beta_\ell^3 & \text{for } \varphi = h, H \\ \beta_\ell & \text{for } \varphi = A \end{cases}, \quad (\text{A2})$$

$$\Gamma(H^\pm \rightarrow u\bar{d}) = N_C \frac{G_F m_{H^\pm} |V_{ud}|^2}{4\sqrt{2}\pi} \beta_{ud} \left\{ \left(m_u^2 \xi_A^{u^2} + m_d^2 \xi_A^{d^2} \right) \left(1 - \frac{m_u^2 + m_d^2}{m_{H^\pm}^2} \right) - \frac{4m_u^2 m_d^2 \xi_A^u \xi_A^d}{m_{H^\pm}^2} \right\}, \quad (\text{A3})$$

$$\Gamma(H^\pm \rightarrow \ell^+ \nu) = \frac{G_F m_{H^\pm} m_\ell^2}{4\sqrt{2}\pi} \xi_A^{\ell^2} \left(1 - \frac{m_\ell^2}{m_{H^\pm}^2} \right)^2, \quad (\text{A4})$$

where the factors ξ_φ^f are defined in Eq. (6), $q = u, d, s, c, t, b$; $\ell = e, \mu, \tau$; $N_C (= 3)$ is the color factor; V_{ud} is the Kobayashi-Maskawa matrix; and

$$\lambda(x, y) = 1 + x^2 + y^2 - 2x - 2y - 2xy, \quad (\text{A5})$$

$$\beta_X = \lambda^{1/2} \left(\frac{m_X^2}{m_\varphi^2}, \frac{m_X^2}{m_\varphi^2} \right) = \sqrt{1 - \frac{4m_X^2}{m_\varphi^2}}, \quad (\text{A6})$$

$$\beta_{XY} = \lambda^{1/2} \left(\frac{m_X^2}{m_\varphi^2}, \frac{m_Y^2}{m_\varphi^2} \right). \quad (\text{A7})$$

Formulas for the decay widths for loop induced decays are given by

$$\Gamma(\varphi \rightarrow \gamma\gamma) = \frac{G_F \alpha_{\text{EM}}^2 m_\varphi^3}{128\sqrt{2}\pi^3} \left| \sum_f Q_f^2 I_f^\varphi(m_f, N_C) + I_W^\varphi + I_{H^\pm}^\varphi \right|^2, \quad (\text{A8})$$

$$\Gamma(\varphi \rightarrow Z\gamma) = \frac{G_F \alpha_{\text{EM}}^2 m_\varphi^3}{64\sqrt{2}\pi^3} \left(1 - \frac{m_Z^2}{m_\varphi^2} \right)^3 \left| \sum_f Q_f J_f^\varphi(m_f, N_C) + J_W^\varphi + J_{H^\pm}^\varphi \right|^2, \quad (\text{A9})$$

$$\Gamma(\varphi \rightarrow gg) = \frac{G_F \alpha_S^2 m_\varphi^3}{64\sqrt{2}\pi^3} \left| \sum_{f=q} I_f^\varphi(m_f, 1) \right|^2, \quad (\text{A10})$$

where fermionic loop functions are given by

$$I_f^\varphi(m_f, N_C) = \xi_\varphi^f \times \begin{cases} -N_C \frac{4m_f^2}{m_\varphi^2} [2 - \beta_f^2 m_\varphi^2 C_0(0, 0, m_\varphi^2, m_f^2, m_f^2, m_f^2)] & \text{for } \varphi = h, H \\ +4N_C m_f^2 C_0(0, 0, m_\varphi^2, m_f^2, m_f^2, m_f^2) & \text{for } \varphi = A \end{cases}, \quad (\text{A11})$$

$$J_f^\varphi(m_f, N_C) = \xi_\varphi^f \times \begin{cases} -4N_C c_V^f [J_1(m_f) - J_2(m_f)] & \text{for } \varphi = h, H \\ -4N_C c_V^f [-J_2(m_f)] & \text{for } \varphi = A \end{cases}, \quad (\text{A12})$$

and

$$J_1(m) = \frac{2m^2}{m_\varphi^2 - m_Z^2} \left\{ 1 + 2m^2 C_0(0, m_Z^2, m_\varphi^2, m^2, m^2, m^2) + \frac{m_Z^2}{m_\varphi^2 - m_Z^2} [B_0(m_\varphi^2, m^2, m^2) - B_0(m_Z^2, m^2, m^2)] \right\}, \quad (\text{A13})$$

$$J_2(m) = m^2 C_0(0, m_Z^2, m_\varphi^2, m^2, m^2, m^2), \quad (\text{A14})$$

with $c_V^f = \frac{1}{2s_W c_W} (T_{3L}^f - 2Q_f s_W^2)$, where T_{3L}^f is the third component of the isospin. The functions B_0 and C_0 are the Passarino-Veltman functions [71], which can be expressed by analytic functions as

$$B_0(m_\varphi^2, m^2, m^2) = \Delta - 2g \left(\frac{4m^2}{m_\varphi^2} \right) \quad (\text{A15})$$

$$B_0(m_Z^2, m^2, m^2) = \Delta - 2g \left(\frac{4m^2}{m_Z^2} \right) \quad (\text{A16})$$

$$C_0(0, 0, m_\varphi^2, m^2, m^2, m^2) = \frac{-2}{m_\varphi^2} f \left(\frac{4m^2}{m_\varphi^2} \right) \quad (\text{A17})$$

$$C_0(0, m_Z^2, m_\varphi^2, m^2, m^2, m^2) = \frac{-2}{m_\varphi^2 - m_Z^2} \left[f \left(\frac{4m^2}{m_\varphi^2} \right) - f \left(\frac{4m^2}{m_Z^2} \right) \right] \quad (\text{A18})$$

where Δ denotes the regularized divergence part in the dimensional regularization, and

$$g(x) = \begin{cases} (x-1) \arcsin(\sqrt{1/x}) & \text{for } x \geq 1 \\ \frac{1}{2}(1-x) \left[\ln \left(\frac{1+\sqrt{1-x}}{1-\sqrt{1-x}} \right) - i\pi \right] & \text{for } x < 1 \end{cases}, \quad (\text{A19})$$

$$f(x) = \begin{cases} \left[\arcsin(\sqrt{1/x}) \right]^2 & \text{for } x \geq 1 \\ -\frac{1}{4} \left[\ln \left(\frac{1+\sqrt{1-x}}{1-\sqrt{1-x}} \right) - i\pi \right]^2 & \text{for } x < 1 \end{cases}. \quad (\text{A20})$$

The loop functions I_W, I_{H^\pm}, J_W and J_{H^\pm} are common among all types of Yukawa interactions, which can be found in Ref. [2].

-
- [1] ATLAS Collaboration, <http://atlas.web.cern.ch/Atlas/>; CMS Collaboration, <http://cms.cern.ch/>.
 - [2] For the review, J. F. Gunion, H. E. Haber, G. Kane and S. Dawson, *The Higgs Hunter's Guide* (Frontiers in Physics series, Addison-Wesley, 1990); A. Djouadi, *Phys. Rept.* **459**, 1 (2008).
 - [3] H. J. He, C. T. Hill and T. M. P. Tait, *Phys. Rev. D* **65**, 055006 (2002). B. Holdom, *JHEP* **0608**, 076 (2006).
 - [4] A. Zee, *Phys. Lett. B* **93**, 389 (1980) [Erratum-ibid. *B* **95**, 461 (1980)]; R. N. Mohapatra and G. Senjanovic, *Phys. Rev. Lett.* **44**, 912 (1980); J. Schechter and J. W. F. Valle, *Phys. Rev. D* **22**, 2227 (1980); G. B. Gelmini and M. Roncadelli, *Phys. Lett. B* **99**, 411 (1981); A. Zee, *Phys. Lett. B* **161**, 141 (1985). L. M. Krauss, S. Nasri and M. Trodden, *Phys. Rev. D* **67**, 085002 (2003). E. Ma, *Phys. Rev. D* **73**, 077301 (2006); N. Sahu and U. Sarkar, *Phys. Rev. D* **76**, 045014 (2007); K. S. Babu and E. Ma, *Int. J. Mod. Phys. A* **23**, 1813 (2008). N. Sahu and U. Sarkar, *Phys. Rev. D* **78**, 115013 (2008).
 - [5] J. McDonald, *Phys. Rev. D* **50** (1994) 3637; R. Barbieri, L. J. Hall and V. S. Rychkov, *Phys. Rev. D* **74**, 015007 (2006); M. Cirelli, N. Fornengo and A. Strumia, *Nucl. Phys. B* **753**, 178 (2006).
 - [6] A.G. Cohen, D.B. Kaplan, A.E. Nelson, *Ann. Rev. Nucl. Part. Sci.* **43** (1993) 27; A.T. Davies, C.D. Froggatt, G. Jenkins, R.G. Moorhouse, *Phys. Lett. B* **336** (1994) 464; K. Funakubo, A. Kakuto, K. Takenaga, *Prog. Theor. Phys.* **91** (1994) 341; J.M. Cline, K. Kainulainen, A.P. Vischer, *Phys. Rev. D* **54** (1996) 2451; S. Kanemura, Y. Okada and E. Senaha, *Phys. Lett. B* **606** (2005) 361, L. Fromme, S. J. Huber and M. Seniuch, *JHEP* **0611**, 038 (2006).
 - [7] M. Aoki, S. Kanemura, O. Seto, *Phys. Rev. Lett.* **102**, 051805 (2009).
 - [8] B. W. Lee, *Proceedings of the XVI International Conference on High Energy Physics*, Batavia, IL (1972), ed. J. D. Jackson, A. Roberts and R. Donaldson, Vol. 4; D. A. Ross and M. J. G. Veltman, *Nucl. Phys. B* **95**, 135 (1975); H.-S. Tsao, in *Proceedings of the 1980 Guanzhou Conference on Theoretical Particle Physics*, edited by H. Ning and T. Hung-yuan, (Science Press, Beijing, 1980) p.1240; P. Sikivie, L. Susskind, M. B. Voloshin and V. I. Za-

- kharov, Nucl. Phys. B **173**, 189 (1980).
- [9] S. L. Glashow, J. Iliopoulos and L. Maiani, Phys. Rev. D **2**, 1285 (1970).
 - [10] S. L. Glashow and S. Weinberg, Phys. Rev. D **15**, 1958 (1977).
 - [11] V. D. Barger, J. L. Hewett and R. J. N. Phillips, Phys. Rev. D **41**, 3421 (1990).
 - [12] Y. Grossman, Nucl. Phys. B **426**, 355 (1994).
 - [13] A. G. Akeroyd and W. J. Stirling, Nucl. Phys. B **447**, 3 (1995); A. G. Akeroyd, Phys. Lett. B **377**, 95 (1996); J. Phys. G **24**, 1983 (1998).
 - [14] J. Liu and L. Wolfenstein, Nucl. Phys. B **289**, 1 (1987).
 - [15] ILC Collaboration, <http://www.linearcollider.org/cms/>.
 - [16] ALEPH, DELPHI, L3 and OPAL Collaborations, The LEP Working Group for Higgs Boson Searches, Phys. Lett. B **565**, 61 (2003); Eur. Phys. J. C **47**, 547 (2006).
 - [17] A. Abulencia *et al.* [CDF Collaboration], Phys. Rev. Lett. **96**, 042003 (2006); V. M. Abazov *et al.* [D0 Collaboration], Phys. Rev. Lett. **88**, 151803 (2002).
 - [18] M. Ciuchini, G. Degrossi, P. Gambino and G. F. Giudice, Nucl. Phys. B **527**, 21 (1998).
 - [19] P. Ciafaloni, A. Romanino and A. Strumia, Nucl. Phys. B **524**, 361 (1998); F. Borzumati and C. Greub, Phys. Rev. D **58**, 074004 (1998); T. M. Aliev and E. O. Iltan, Phys. Rev. D **58**, 095014 (1998).
 - [20] M. Misiak and M. Steinhauser, Nucl. Phys. B **764**, 62 (2007).
 - [21] M. Misiak *et al.*, Phys. Rev. Lett. **98**, 022002 (2007); T. Becher and M. Neubert, Phys. Rev. Lett. **98**, 022003 (2007).
 - [22] A. G. Akeroyd and S. Recksiegel, J. Phys. G **29**, 2311 (2003); M. Krawczyk and D. Sokolowska, *In the Proceedings of 2007 International Linear Collider Workshop*, , pp *HIG09*, arXiv:0711.4900 [hep-ph].
 - [23] D. s. Du, arXiv:0709.1315 [hep-ph].
 - [24] M. Krawczyk and D. Temes, Eur. Phys. J. C **44**, 435 (2005).
 - [25] R. Jackiw and S. Weinberg, Phys. Rev. D **5**, 2396 (1972); K. Fujikawa, B. W. Lee and A. I. Sanda, Phys. Rev. D **6**, 2923 (1972).
 - [26] J. P. Leveille, Nucl. Phys. B **137**, 63 (1978); H. E. Haber, G. L. Kane and T. Sterling, Nucl. Phys. B **161**, 493 (1979); M. Krawczyk and J. Zochowski, Phys. Rev. D **55**, 6968 (1997); A. Dedes and H. E. Haber, JHEP **0105**, 006 (2001).
 - [27] N. G. Deshpande and E. Ma, Phys. Rev. D **18**, 2574 (1978); M. Sher, Phys. Rept. **179**, 273

- (1989).
- [28] S. Nie and M. Sher, Phys. Lett. B **449**, 89 (1999); S. Kanemura, T. Kasai and Y. Okada, Phys. Lett. B **471**, 182 (1999).
 - [29] B. W. Lee, C. Quigg and H. B. Thacker, Phys. Rev. D **16**, 1519 (1977).
 - [30] S. Kanemura, T. Kubota and E. Takasugi, Phys. Lett. B **313**, 155 (1993).
 - [31] H. Huffel and G. Pocsik, Z. Phys. C **8**, 13 (1981); J. Maalampi, J. Sirkka and I. Vilja, Phys. Lett. B **265**, 371 (1991); A. G. Akeroyd, A. Arhrib and E. M. Naimi, Phys. Lett. B **490**, 119 (2000); I. F. Ginzburg and I. P. Ivanov, arXiv:hep-ph/0312374, Phys. Rev. D **72**, 115010 (2005).
 - [32] J. F. Gunion and H. E. Haber, Phys. Rev. D **67**, 075019 (2003).
 - [33] S. Kanemura, Y. Okada, E. Senaha and C. P. Yuan, Phys. Rev. D **70**, 115002 (2004).
 - [34] S. Kanemura, S. Moretti, Y. Mukai, R. Santos and K. Yagyu, arXiv:0901.0204 [hep-ph].
 - [35] H. E. Haber and A. Pomarol, Phys. Lett. B **302**, 435 (1993); A. Pomarol and R. Vega, Nucl. Phys. B **413**, 3 (1994).
 - [36] P. H. Chankowski, M. Krawczyk and J. Zochowski, Eur. Phys. J. C **11**, 661 (1999); W. Grimus, L. Lavoura, O. M. Ogreid and P. Osland, Nucl. Phys. B **801**, 81 (2008).
 - [37] A. Abulencia *et al.* [CDF Collaboration], Phys. Rev. Lett. **96**, 042003 (2006); M. Baarmand, M. Hashemi and A. Nikitenko, J. Phys. G **32**, N21 (2006).
 - [38] A. Czarnecki and S. Davidson, Phys. Rev. D **47**, 3063 (1993); A. Czarnecki and S. Davidson, Phys. Rev. D **48**, 4183 (1993).
 - [39] K. Abe *et al.* [Belle Collaboration], AIP Conf. Proc. **1078**, 342 (2009)
 - [40] B. Aubert *et al.* [BABAR Collaboration], Phys. Rev. D **77**, 051103 (2008).
 - [41] S. Chen *et al.* [CLEO Collaboration], Phys. Rev. Lett. **87**, 251807 (2001).
 - [42] C. Amsler *et al.* [Particle Data Group], “Review of particle physics,” Phys. Lett. B **667**, 1 (2008).
 - [43] E. Barberio *et al.* [Heavy Flavor Averaging Group], arXiv:0808.1297 [hep-ex].
 - [44] T. Goto and Y. Okada, Prog. Theor. Phys. **94**, 407 (1995); M. Ciuchini, G. Degrossi, P. Gambino and G. F. Giudice, Nucl. Phys. B **534**, 3 (1998).
 - [45] B. Aubert *et al.* [BABAR Collaboration], Phys. Rev. D **77**, 011107 (2008).
 - [46] G. Isidori and P. Paradisi, Phys. Lett. B **639**, 499 (2006).
 - [47] S. M. Barr and A. Zee, Phys. Rev. Lett. **65**, 21 (1990) [Erratum-ibid. **65**, 2920 (1990)].

- [48] D. Chang, W. F. Chang, C. H. Chou and W. Y. Keung, Phys. Rev. D **63**, 091301 (2001); K. m. Cheung, C. H. Chou and O. C. W. Kong, Phys. Rev. D **64**, 111301 (2001); K. Cheung and O. C. W. Kong, Phys. Rev. D **68**, 053003 (2003).
- [49] A. C. Bawa, C. S. Kim and A. D. Martin, Z. Phys. C **47**, 75 (1990); J. L. Diaz-Cruz and O. A. Sampayo, Phys. Rev. D **50**, 6820 (1994); V. D. Barger, R. J. N. Phillips and D. P. Roy, Phys. Lett. B **324**, 236 (1994); L. G. Jin, C. S. Li, R. J. Oakes and S. H. Zhu, Eur. Phys. J. C **14**, 91 (2000); A. Belyaev, D. Garcia, J. Guasch and J. Sola, JHEP **0206**, 059 (2002); T. Plehn, Phys. Rev. D **67**, 014018 (2003); J. Alwall and J. Rathsmann, JHEP **0412**, 050 (2004); S. h. Zhu, Phys. Rev. D **67**, 075006 (2003); E. L. Berger, T. Han, J. Jiang and T. Plehn, Phys. Rev. D **71**, 115012 (2005); K. A. Assamagan and N. Gollub, Eur. Phys. J. C **39S2**, 25 (2005).
- [50] J. F. Gunion, H. E. Haber, F. E. Paige, W. K. Tung and S. S. D. Willenbrock, Nucl. Phys. B **294**, 621 (1987);
- [51] S. S. D. Willenbrock, Phys. Rev. D **35**, 173 (1987); O. Brein and W. Hollik, Eur. Phys. J. C **13**, 175 (2000); A. A. Barrientos Bendezu and B. A. Kniehl, Phys. Rev. D **64**, 035006 (2001).
- [52] J. F. Gunion and H. E. Haber, Nucl. Phys. B **278**, 449 (1986).
- [53] D. A. Dicus, J. L. Hewett, C. Kao and T. G. Rizzo, Phys. Rev. D **40**, 787 (1989); S. Moretti and K. Odagiri, Phys. Rev. D **59**, 055008 (1999); A. A. Barrientos Bendezu and B. A. Kniehl, Phys. Rev. D **59**, 015009 (1998); O. Brein, W. Hollik and S. Kanemura, Phys. Rev. D **63**, 095001 (2001); W. Hollik and S. h. Zhu, Phys. Rev. D **65**, 075015 (2002); E. Asakawa, O. Brein and S. Kanemura, Phys. Rev. D **72**, 055017 (2005); D. Eriksson, S. Hesselbach and J. Rathsmann, Eur. Phys. J. C **53**, 267 (2008).
- [54] H. M. Georgi, S. L. Glashow, M. E. Machacek and D. V. Nanopoulos, Phys. Rev. Lett. **40**, 692 (1978).
- [55] R. N. Cahn and S. Dawson, Phys. Lett. B **136**, 196 (1984) [Erratum-ibid. B **138**, 464 (1984)]; D. A. Dicus and S. S. D. Willenbrock, Phys. Rev. D **32**, 1642 (1985); G. Altarelli, B. Mele and F. Pitolli, Nucl. Phys. B **287**, 205 (1987).
- [56] D. L. Rainwater and D. Zeppenfeld, JHEP **9712**, 005 (1997); D. L. Rainwater, D. Zeppenfeld and K. Hagiwara, Phys. Rev. D **59**, 014037 (1998).
- [57] S. Dawson, C. B. Jackson, L. Reina and D. Wackeroth, Phys. Rev. D **69**, 074027 (2004); S. Dittmaier, M. I. Kramer and M. Spira, Phys. Rev. D **70**, 074010 (2004); J. M. Campbell

- et al.*, arXiv:hep-ph/0405302.
- [58] R. Raitio and W. W. Wada, Phys. Rev. D **19**, 941 (1979); J. N. Ng and P. Zakarauskas, Phys. Rev. D **29**, 876 (1984); A. S. Bagdasaryan, R. S. Egorian, S. G. Grigorian and S. G. Matinyan, Sov. J. Nucl. Phys. **46**, 315 (1987) [Yad. Fiz. **46**, 572 (1987)]; D. A. Dicus, C. Kao and S. S. D. Willenbrock, Phys. Lett. B **203**, 457 (1988).
 - [59] Z. Kunszt, Nucl. Phys. B **247**, 339 (1984).
 - [60] “ATLAS detector and physics performance. Technical Design Report. Vol. 2,” , ATLAS-TDR-015, CERN-LHCC-99-015; G. Aad *et al.* [The ATLAS Collaboration], arXiv:0901.0512.
 - [61] T. Han and B. McElrath, Phys. Lett. B **528**, 81 (2002).
 - [62] S. Kanemura and C. P. Yuan, Phys. Lett. B **530** 188 (2002).
 - [63] A. G. Akeroyd, Phys. Rev. D **68** (2003) 077701.
 - [64] Q. H. Cao, S. Kanemura and C. P. Yuan, Phys. Rev. D **69**, 075008 (2004).
 - [65] Q. H. Cao, D. Nomura, K. Tobe and C. P. Yuan, Phys. Lett. B **632**, 688 (2006); A. Belyaev, Q. H. Cao, D. Nomura, K. Tobe and C. P. Yuan, Phys. Rev. Lett. **100**, 061801 (2008).
 - [66] A. Pukhov, arXiv:hep-ph/0412191.
 - [67] J. F. Gunion *et al.*, Phys. Rev. D **38**, 3444 (1988); A. Djouadi, J. Kalinowski and P. M. Zerwas, Z. Phys. C **57**, 569 (1993).
 - [68] V. Barger, H. E. Logan and G. Shaughnessy, arXiv:0902.0170 [hep-ph].
 - [69] H. S. Goh, L. J. Hall and P. Kumar, arXiv:0902.0814 [hep-ph].
 - [70] D. Eriksson, J. Rathsmann and O. Stal, arXiv:0902.0851 [hep-ph].
 - [71] G. Passarino and M. J. G. Veltman, Nucl. Phys. B **160**, 151 (1979).